Journal of Engineering Mathematics (2006) 55: 313–338
DOI 10.1007/s10665-006-9043-4

Basic properties of free stratified flows

YULI D. CHASHECHKIN, VASILIY G. BAYDULOV,
ANATOLIY V. KISTOVICH
Laboratory of Fluid Mechanics, Institute for Problems in Mechanics of the RAS 101/1 prospect Vernadskogo, Moscow, 119526, Russia (E-mail: chakin@ipmnet.ru)

Received 11 March 2004; accepted in revised form 14 February 2006 / Published online: 14 July 2006

Abstract. Results of analytical studies of the governing equations of stratified rotating fluids based on the unification of theories of continuous and discrete groups, perturbations and modern numerical visualizations are described. Symmetries of basic systems and their simplified versions, different approximations and constitutive turbulent models are compared. A new method to calculate discrete groups analytically, which does not need a preliminary search for continuous groups, is developed. As an example of the practical use of the developed algorithm, a complete classification of cellular and roll structures of Bénard convection is presented. A complete classification of 3D periodic motions in compressible viscous stratified and rotating fluids, including regular (wave) and singular elements, is performed by perturbation methods. In all cases, in a viscous fluid, besides waves there are two different periodic boundary layers. In a homogeneous fluid the split boundary layers are merged, thus forming a joint doubly-degenerate structure. Stratification and rotation reduce the degeneration of the 3D periodic boundary layers. Calculations of a 3D periodic wave beam emitted by an oscillating part of a sloping plane are visualized by a computer-graphics method. The existence of thin extended components on the edges of the 3D wave cone is demonstrated.

Key words: boundary layers, complete equations, continuous and discrete groups, exact solutions, internal waves

1. Introduction

The study of stratified flows is motivated logically by the historical evolution of theoretical fluid mechanics and by a wide class of different technological and environmental applications. In a model that was first developed for an ideal fluid, the drag of a body could not be calculated for more than 100 years, as it does not fit the experimental data. The introduction of viscosity effects in theoretical fluid dynamics allows the solution of a wide range of laminar-flow problems but cannot solve the important problem of instability and turbulence. In the environment, fluids are placed on a rotating spherical planet and are mostly stratified due to the nonuniformity of the temperature or concentration fields of dissolved and suspended matter. Stratification and rotation, even if very weak, lead to certain new phenomena that are not present in a homogeneous environment at rest. Among these phenomena there are inertial and internal waves and so-called 'large scale' and 'fine' structures. The general circulation of the Earth's atmosphere manifests itself in counter-moving large-scale cells in the latitudinal direction. The fine structure results in thin high-gradient interfaces, mostly in a vertical direction. Extended, almost horizontal, interfaces separate thicker and more homogeneous layers in the ocean and in the Earth's atmosphere. Boundaries between jets, vortices, vortex systems and convective cells are marked by sharp interfaces in a horizontal plane. Thin interfaces exist for rather a long time, that is, much longer than the specific diffusion time for the given lengthscale. They produce picturesque patterns of environmental flows and their laboratory models.

Satellite observations reveal similarity in the general shapes and differences in the details of flow patterns in the Earth's atmosphere and the ocean containing elements with gradual and discrete variations of the basic parameters. Cloud patterns in the atmosphere reveal jets, wakes, stagnation areas and discrete cells produced by moisture convection above the ocean. Cloud streets sometimes reveal a high degree of order and, at other times, chaotic disorder, but the boundaries between the flow elements remain very sharp. The thickness of a boundary is small with respect to the size of flow elements. These experimental facts should be taken into account when analyzing basic mathematical models for environmental processes.

Because of the complexity of the governing fluid-dynamic equations, they are substituted by simpler ones, and the degree of correspondence between the initial and the reduced systems cannot be assessed analytically. Fortunately, progress in computer hard- and software techniques gives the opportunity of a practical realization of well-known mathematical methods with relatively simple algorithms but involving extremely large calculations. Among these analytic methods there is the theory of continuous (Lie) groups, high-order perturbation theory, asymptotic calculations and a new regular method of calculation that exploits discrete symmetries of flows. Further development of these techniques enable one to construct exact (on limiting space-time intervals) models in fluid mechanics. These advanced models allow one to calculate all the varieties of the flow parameters described by nonlinear equations with a prescribed accuracy directly or using exact solutions of their linearized residuals satisfying real boundary conditions. The main goal of the paper is to present an algorithm for an objective comparison of different models and to illustrate its efficiency by examples of exact solutions of the 3D internal-waves-generation problem.

The plan for this paper is to discuss briefly the properties of the governing equations employed in Section 2. Comparative analyses of point symmetries by Lie-groups methods for different models of rotating and stratified flows (sets with the Navier–Stokes equation, turbulence models) are presented in Section 3. A new method for the calculation of discrete symmetries of differential equations is given in Section 4. As an example, calculations of possible flow patterns in Bénard convection, based on discrete symmetries, are employed in Section 5. A complete classification of infinitesimal periodic motions of fluid, taking into account both regular (waves) and singular (set of boundary layers) components of motion, is presented in Section 6. The generation of 3D periodic internal waves by a compact oscillating source on a rigid plane is discussed in Section 7 as an example of the construction of an exact solution. A summary of results and some concluding remarks are given in Section 8. A part of the results has been published in a number of papers in the Russian journal Doklady Physics oriented towards a brief urgent publication of scientific results. The status of the journal supposes independent publication of extended versions of these papers.

2. Basic systems of governing equations

We analyze the general property of two types of equation in geophysical fluid-dynamics equation sets used to investigate large-scale and small-scale phenomena. We neglect the effects of compressibility in this part of the paper. Large-scale fluid phenomena are studied for a spherical planet rotating at an angular velocity Ω with a gravity field characterized by an acceleration g. The density profile is defined by the salinity S of the concentration of dissolved or dispersed matter and described by an algebraic equation of state. In general, an undisturbed density profile $\rho(z)$ is characterized by the buoyancy scale $\Lambda = (\mathrm{d}\log\rho(z)/\mathrm{d}z)^{-1}$ and buoyancy frequency $N = \sqrt{g/\Lambda}$, which can be assumed constant.

The set of governing equations is [1]

$$\begin{aligned}
&\rho(S)\left(\frac{\partial \mathbf{v}}{\partial t}+(\mathbf{v}\nabla)\,\mathbf{v}\right)=-\nabla P+\nabla\left(\mu(S)\nabla\mathbf{v}\right)+\rho(S)\;(\mathbf{g}-2\Omega\times\mathbf{v}),\\
&\frac{\partial S}{\partial t}+(\mathbf{v}\nabla)\,S=\nabla\left(\kappa_S(S)\nabla S\right),\\
&\operatorname{div}\,\mathbf{v}=0,\quad \rho=\rho(S),
\end{aligned}\tag{2.1}$$

where $\mathbf{v}=(u,v,w)$ is the velocity of the fluid, P is the total pressure, $\rho=\rho(S)$ is the density of the fluid, μ and $\nu=\mu/\rho$ are the dynamic and kinematic viscosity, κ_S is the salt-diffusion coefficient, the salt-contraction coefficient being included in the definition of the salinity S, which is a dimensionless variable. The set (2.1) consists of nonlinear differential equations and an algebraic equation of state. These nonlinear differential equations are of a singularly perturbed type and contain small coefficients in the high-order terms. In particular cases the set (2.1) must be supplemented by initial and boundary conditions. In practical cases one can use different simplified or model systems instead of the complex set (2.1).

In the environment, variations of density usually are small and in (2.1) can be neglected everywhere, except for the buoyancy-force term including the large coefficient g. In this so-called Boussinesq approximation the first equation of (2.1) is transformed into the following (other equations of the set remain unchanged):

$$\frac{\partial \mathbf{v}}{\partial t}+(\mathbf{v}\nabla)\;\mathbf{v}=-\frac{1}{\rho_0}\nabla P'+\nabla\left(\nu(S)\,\nabla\mathbf{v}\right)+\rho'(S)\mathbf{g}-2\Omega\times\mathbf{v},\tag{2.2}$$

where $\rho'=(\rho-\rho_0)/\rho_0$ is the relative density variation, ρ_0 is a reference density, P' is the variation of the pressure.

For solutions of practically important problems, instead of the set (2.1), different derivatives and constitutive models are used. Due to relative-scale differences, effects of rotation and stratification are analyzed separately [2, 3]. A natural instrument to compare properties of different models is a comparison of their continuous symmetries defined by Lie-groups methods [4, 5] and discrete symmetries.

Searching for Lie groups of the complex set of partial differential equations (PDE) includes a large number of routine calculations, which can now be evaluated by means of computer algebra. The algorithm for searching Lie-group generators is written in Maple. Different procedures are used to control the calculations and to check the constructed symmetry group by direct insertion into the set of governing equations.

Using the linearized equation of state and the usual approximations of constant viscosity and diffusivity, we calculated the basic infinite-dimensional group of symmetry of the set (2.1) with approximation (2.2). The set of governing equations is written in the spherical co-ordinate frame $(r,\vartheta,\varphi): x=r\sin\vartheta\cos\varphi,\ y=r\sin\vartheta\sin\varphi,\ z=r\cos\vartheta$; where Ω is directed along the axis Oz and acceleration due to gravity is directed along the radius-vector $\mathbf{g}=-g\mathbf{e_r}$. As the fluid is placed into a centrally symmetric gravity field, the problem space becomes non-uniform and space-translation symmetry is lost. This is a basic principle of classical mechanics—the Galilean relativity principle is also violated for the same reason. So the basis of the generators for the symmetry group of the set (2.1) with (2.2) includes the following operators:

$X_1=\partial_t$ (time translations);

$X_\pi=\pi(t)\partial_P;\quad X_3=\partial_S-gr\,\partial_P$ (pressure, mutual pressure and salinity shifts);

$$X_2=2t\partial_t+r\partial_r-2\Omega t\partial_\varphi-v\partial_v-u\partial_u-(2\Omega r\sin\vartheta+w)\,\partial_w-3S\partial_S-2\left(P+r^2\Omega^2\sin^2\vartheta\right)\partial_P$$

(modified expansions);

$$X_4 = \partial_\varphi \text{ (rotations around the axis } Oz);$$

$$X_5 = -2\cos\tilde{\varphi}\partial_\vartheta + 2\operatorname{cotan}\vartheta\sin\tilde{\varphi}\,\partial_\varphi + 2\sin\tilde{\varphi}\left(r\,\Omega + \frac{1}{\sin\vartheta}w\right)\partial_u + \\ + 2\left(r\,\Omega\cos\vartheta\cos\tilde{\varphi} - \frac{1}{\sin\vartheta}u\sin\tilde{\varphi}\right)\partial_w + (r\,\Omega)^2\sin 2\vartheta\cos\tilde{\varphi}\partial_P \tag{2.3}$$

(rotations around the axis $O\tilde{y}$);

$$X_6 = 2\sin\tilde{\varphi}\,\partial_\vartheta + 2\operatorname{cotan}\vartheta\cos\tilde{\varphi}\,\partial_\varphi + \cos\tilde{\varphi}\left(r\,\Omega + \frac{2}{\sin\vartheta}w\right)\partial_u - \\ - \left(r\,\Omega\cos\vartheta\sin\tilde{\varphi} + \frac{2}{\sin\vartheta}u\cos\tilde{\varphi}\right)\partial_w - (r\,\Omega)^2\sin 2\vartheta\sin\tilde{\varphi}\,\partial_P$$

(rotations around the axis $O\tilde{x}$);
where $\tilde{\varphi} = \varphi + \Omega t$, $r\sin\vartheta\sin\tilde{\varphi} = \tilde{y} = \text{inv}$, $r\sin\vartheta\cos\tilde{\varphi} = \tilde{x} = \text{inv}$, $\pi(t)$ is an arbitrary function of time.

In a Cartesian co-ordinate plane placed on the north pole of the rotating system with uniform gravity acceleration ($\mathbf{g} = -g\mathbf{e}_z$) generators the groups of symmetries are:

$$X_1 = \partial_t \text{ (time translations);}$$
$$X_\pi = \pi(t)\partial_P; \quad X_3 = \partial_S - gr\partial_P \text{ (pressure, mutual pressure and salinity shifts);}$$

and transformation to an arbitrary rectilinearly moving coordinate system

$$X = X_\chi + X_\eta + X_\zeta, \text{ where}$$
$$X_\chi = \chi(t)\,\partial_x + \dot{\chi}(t)\,\partial_u - (\ddot{\chi}(t)x + \dot{\chi}(t)\Omega y)\,\partial_P; \tag{2.4}$$
$$X_\eta = \eta(t)\,\partial_y + \dot{\eta}(t)\,\partial_v - (\ddot{\eta}(t)y - \dot{\eta}(t)\Omega x)\,\partial_P;$$
$$X_\zeta = \zeta(t)\,\partial_z + \dot{\zeta}(t)\,\partial_w - \ddot{\zeta}(t)z\partial_P.$$

The description of the fine structure of the atmosphere and ocean reveals that density gradients in environmental flows can be relatively large in small-scale phenomena that are not affected by centripetal and Coriolis forces. In this context it is necessary to compare Lie-group symmetries of the governing equations in the common case and in the Boussinesq approximation.

The general set (2.1) with $\Omega = 0$ is characterized by the group containing the operators

$$X_1 = \partial_t; \quad X_{2\ldots4} = \partial_{x_i} \text{ (time and space translations);}$$
$$X_{5\ldots7} = t\partial_{x_i} + \partial_{u_i} \text{ (Galilean's relativity principle);} \tag{2.5}$$
$$X_8 = y\partial_x - x\partial_y + v\partial_u - u\partial_v \text{ (rotation in the horizontal plane);}$$
$$X_{9,10} = \left(\frac{gt^2}{2} + z\right)\partial_{x_i} - x_i\partial_z + (gt + w)\,\partial_{v_i} - v_i\partial_w$$
(rotations in vertical planes moving with acceleration $\mathbf{g}$)

and infinite-dimensional sub-algebra $X_\pi = \pi(t)\partial_P$, (pressure shifts).

The system (2.1) contains algebraic parts that are equations of state for the density and empirical functions for viscosity and diffusivity coeffiients that can be written in different functional forms. Symmetry groups of the governing equations can be expanded or reduced,

Table 1. Additional symmetry properties and optimal form of the equation of state.

Additional generators of the set (2.1)	Equation of state
$X_{11} = 2t\partial_t + \mathbf{r}\partial_{\mathbf{r}} - \mathbf{v}\partial_{\mathbf{v}} - \frac{3gt}{2}(t\partial_z + 2\partial_w) - 2P\partial_P$	$\boldsymbol{\rho}'$ is arbitrary function of salinity.
$X_{11} = 2t\partial_t + \mathbf{r}\partial_{\mathbf{r}} - \mathbf{v}\partial_{\mathbf{v}} - \frac{3gt}{2}(t\partial_z + 2\partial_w) + 2\rho\partial_\rho$, $X_{12} = P\partial_P + \rho\partial_\rho$	$\rho' = (a_0 + a_1 S)^{-b/a_1}$, $\rho' = \exp(-b/a_0 S)$, a_0, a_1 and b are arbitrary constants.

depending on the functional form of these values. Expansion of the symmetry group extends the level at which the governing equations can be analyzed (2.1). Additional symmetries expanding the basic symmetries (2.5), which are available for any equation of state, are presented in Table 1. These conditions prescribe the choice of the most constructive form of the empirical equation of state [6].

In the Boussinesq approximation for (2.1), with the Navier–Stokes equations in the form of (2.2), the basic symmetry group includes a general part which does not depend on the form of the algebraic equation of state. Thus we have

$X_1 = \partial_t$ (time translation);

$X_2 = y\partial_x - x\partial_y + v\partial_u - u\partial_v$ (rotation in the horizontal plane);

and infinite-dimensional sub-algebras

$X_\pi = \pi(t)\partial_P$ (pressure shifts)

and a transformation into an arbitrary rectilinearly moving coordinate system

$$X_{\chi_i} = \chi_i(t)\,\partial_{x_i} + \chi_i'(t)\,\partial_{v_i} - \chi_i''(t)\,x_i\,\partial_P, \quad i = \overline{1,3}. \tag{2.6}$$

The most essential transformation of the symmetry properties is to expand the Galilean principle of relativity in a noninertial system moving with an arbitrary rectilinear acceleration. Fictitious inertial forces are compensated by the pressure-force transformations. This condition, which is a sequence of the differences between the inertial and gravitational masses, leads to preserving the form of the governing equations.

This symmetry was first found for the equations of an inviscid incompressible homogeneous liquid (Euler equations). The study of stratified flows provides a basis for understanding this phenomenon and an instrument for its practical use in theoretical fluid mechanics.

A wide class of models with negligible diffusion effects ($\kappa_S = 0, \nu \neq 0$) is characterized by a continuous dependence of symmetry groups on the state equation ($\rho = \rho(S)$). In all models of this kind the basic symmetry group is expanded and the algebra of the generators is supplemented by additional generators. A new operator for the complete system (2.1) is

$X_3 = 2t\partial_t + \mathbf{r}\partial_{\mathbf{r}} - \mathbf{v}\partial_{\mathbf{v}} - 2P\partial_P - 3\rho\partial_\rho$ (expansion),

and the ones for the Boussinesq system (2.2) are

$X_{11} = 2t\partial_t + \mathbf{r}\partial_{\mathbf{r}} - \mathbf{v}\partial_{\mathbf{v}} - \frac{3gt}{2}(t\partial_z + 2\partial_w) + 2\rho\partial_\rho$ (combined symmetry),

$X_{12} = \rho\partial_\rho + P\partial_P$ (expansion),

where $\rho\partial_\rho = \rho\,(\partial\rho/\partial S)^{-1}\,\partial_S$.

Table 2. Optimal functional representation for the kinetic coefficients and equation of state.

Kinetic coefficients	Equation of state
1. $\nu = \nu_0 (a_0 + a_1 S)^{c/a_1}$, $\kappa_S = \kappa_S^0 (a_0 + a_1 S)^{c/a_1}$	$\rho' = b_0 + b_1 S$
2. $\nu = \nu_0 \exp(cS)$, $\kappa_S = \kappa_S^0 exp(cS)$	$\rho' = \rho_0 \exp(bS)$
3. $\nu = \nu_0 \exp S$, $\kappa_S = \kappa_S^0 \exp(cS)$	$\rho' = b_0 + b_1 S$
4. $\nu = \nu_0 (a_0 + a_1 S)^{c/a_1}$, $\kappa_S = \kappa_S^0 (a_0 + a_1 S)^{c/a_1}$ (only for Boussinesq system)	$\rho' = b_1/a_1 \log(a_0 + a_1 S)$
where $a_0, a_1, b_0, b_1, b, c, \nu_0, \kappa_S^0$ are arbitrary constants	

If the kinetic coefficients in the governing equations (2.1) and (2.2) depend on the salinity, the group analysis selects specific types of equations of state which lead to expansion of the basic symmetry group. In Table 2 specific functions defining the kinetic coefficients and the corresponding type of the equation of state are presented.

In practical fluid mechanics with complex topography, instead of the Navier–Stokes equations, different constitutive models including turbulence models are used. Depending on the closure procedure, a flow described by different sets of governing equations results. One can reveal the basic properties of the models by a Lie-group analysis.

Comparison of the symmetries of the models shows their profound differences. In a central gravity field on a spherical planet, the set (2.1) derived subject to the Boussinesq approximation, besides the rotational symmetry around the axis of rotation Oz, includes two additional symmetries with the generators X_5, X_6 from (2.3) in co-rotation with the planet frame $(\tilde{x}, \tilde{y}, z)$. On a plane-rotating surface in a uniform gravity field, when the frame is a local form of a spherical one, there are no rotational symmetries. The poorest set of generators (2.4) characterizes the plane approximation.

3. Models of turbulent flows

For the description of turbulent flows, a variety of models is constructed. Flows with zero average velocity and finite vorticity, which one can observe past oscillating grids and meshes, are described by the turbulent viscosity coefficient K. The closure condition is selected in the form

$$\overline{\left(v^i \nabla_i\right) v^j} = \nabla_j \overline{\left(v^i v^j\right)} = -\nabla_j K \left(\frac{\partial v^i}{\partial x_j} + \frac{\partial v^j}{\partial x_i} \right), \tag{3.1}$$

where the coefficient K is an empirical function of the spatial co-ordinate. The system of governing equations for averaged values (here and below the sign of averaging is omitted), both for 3D and 2D flows, is

$$\frac{\partial v^i}{\partial t} - \left(\frac{\partial v^i}{\partial x_j} + \frac{\partial v^j}{\partial x_i} \right) \nabla_j K = -\nabla P + K \Delta v_i, \tag{3.2}$$
$$\operatorname{div} \mathbf{v} = 0.$$

Operators of the basic symmetry group for system (3.2) have the form

$$\begin{aligned}
&X_{1\ldots3} = \partial_{x_i} \text{ (spatial shifts)},\\
&X_{4\ldots6} = x^i \partial_{x^j} - x^j \partial_{x^i} + v^i \partial_{v^j} - v^j \partial_{v^i} \text{ (rotations)},\\
&X_7 = \mathbf{r}\partial_{\mathbf{r}} + P\partial_P + K\partial_K, \quad X_8 = \mathbf{v}\,\partial_{\mathbf{v}} + P\,\partial_P \text{ (expansions)},\\
&X_{9\ldots11} = x^i \partial_{v^j} - x^j \partial_{v^i} \text{ (nonuniform shifts of velocity)}.
\end{aligned} \tag{3.3}$$

and infinite-dimensional sub-algebras

$$X = \pi(t)\,\partial_P \text{ (pressure shifts)},$$
$$X_{\varphi_i} = \varphi_i(t)\,\partial_{v_i} - x_i\dot{\varphi}_i(t)\,\partial_P,$$
$$X_\tau = \tau(t)\,\partial_t - \dot{\tau}(t)\,(P\partial_P + K\partial_K) \text{ (generalized shifts and expansions)}.$$

For the given model the basic symmetries are mostly the same as symmetries of the system (2.1) without rotation involving the property of homogeneity and obeying isotropy of space and time, but there are several specific groups of expansions and shifts [6]. At the same time the set of operators (3.3) does not contain the operator of the Galilean transformation, which is fundamental in classical mechanics. There are also additional generators $X_{9\ldots11}$, X_{φ_i} in (3.3), which do not follow from the physical properties of fluid.

To improve the description of the fluid dynamics, more sophisticated closure schemes are developed, including the family of (k–ε) models (k is the turbulent energy, ε is the velocity of turbulent dissipation). To describe the dynamics of a temperature-stratified fluid, the (k–ε–τ–ϑ) model is used (τ is the turbulent Reynolds stress, ϑ is the dispersion of temperature fluctuations [7]). In tensor notation, with summation on repeated indices, the studied set of governing equation is

$$\begin{aligned}
&\operatorname{div}\,\mathbf{v} = 0,\\
&\frac{\mathrm{d}v_i}{\mathrm{d}t} = -\frac{\partial P}{\partial x_i} + \frac{\partial}{\partial x_j}\left(\nu\frac{\partial v_i}{\partial x_j} - w_{ij}\right) + g_i\alpha T,\ \frac{\mathrm{d}T}{\mathrm{d}t} = \frac{\partial}{\partial x_i}\left(\kappa_T\frac{\partial T}{\partial x_i} - q_i\right),\\
&\frac{\mathrm{d}w_{ij}}{\mathrm{d}t} = \frac{\partial}{\partial x_m}\left(\frac{\nu_t}{\sigma_k}\frac{\partial w_{ij}}{\partial x_m}\right) + P_{ij} - \frac{2}{3}\delta_{ij}\varepsilon - c_1\frac{\varepsilon}{k}\left(w_{ij} - \frac{2}{3}\delta_{ij}k\right) - c_2\left(P_{ij} - \frac{2}{3}\delta_{ij}P\right),\\
&\frac{\mathrm{d}k}{\mathrm{d}t} = \frac{\partial}{\partial x_i}\left[\frac{(\nu+\nu_t)}{\sigma_k}\frac{\partial k}{\partial x_i}\right] + \pi - \varepsilon,\\
&\frac{\mathrm{d}q_i}{\mathrm{d}t} = \frac{\partial}{\partial x_j}\left(\frac{\nu_t}{\sigma_\vartheta}\frac{\partial q_i}{\partial x_j}\right) + (1-c_{2T})\,P_{iT} - w_{ij}\frac{\partial T}{\partial x_j} - c_{1T}\frac{\varepsilon}{k}q_i,\\
&\frac{\mathrm{d}\vartheta}{\mathrm{d}t} = \frac{\partial}{\partial x_i}\left(\frac{\nu_t}{\sigma_T}\frac{\partial\vartheta}{\partial x_i}\right) - 2q_i\frac{\partial T}{\partial x_i} - c_T\frac{\varepsilon}{k}\vartheta,\\
&\frac{\mathrm{d}\varepsilon}{\mathrm{d}t} = c_\varepsilon\frac{\partial}{\partial x_i}\left(\frac{\nu_t}{\sigma_\varepsilon}\frac{\partial\varepsilon}{\partial x_i}\right) + c_{\varepsilon1}\frac{\varepsilon}{k}\left(-w_{ij}\frac{\partial v_i}{\partial x_j} + \beta g_i q_i\right) - c_{\varepsilon2}\frac{\varepsilon^2}{k},
\end{aligned} \tag{3.4}$$

where $\mathrm{d}/\mathrm{d}t$ is the substantial derivative; $v_i = \bar{v}_i$, $T = \bar{T}$ and $P = \bar{P}$ are the averaged velocity, temperature and pressure; $w_{ik} = \overline{v_i' v_k'}$, $q_i = \overline{T' v_i'}$, $\vartheta = \overline{T'^2}$ are second-order statistical moments; $\alpha, \kappa_T, \alpha, \kappa_T, \nu$ are $\nu_t = c_\mu k^2/\varepsilon$, are the temperature expansion, heat conductivity, molecular and turbulent kinematic viscosity coefficients, k is kinetic energy of turbulent motions; ε is the rate of turbulent kinetic-energy dissipation; $\Pi = -\overline{v_i' v_k'}\frac{\partial v_i}{\partial x_k}$, $P_{ij} = -w_{im}\frac{\partial v_j}{\partial x_m} - w_{jm}\frac{\partial v_i}{\partial x_m} + \alpha\left(g_i q_j + g_j q_i\right)$, $P_{iT} = -q_j\frac{\partial v_i}{\partial x_j} + \beta g_i\vartheta$ are terms describing turbulent production; $c_1, c_2, c_{1T}, c_{2T}, c_\varepsilon, c_{\varepsilon1}, c_{\varepsilon2}, c_\mu, \sigma_k\,\sigma_\vartheta$ are fitted empirical coefficients.

The very complex set of turbulent Equations (3.4) is characterized by a poor set of symmetries. The set of symmetry-group generators for the system includes

$$X_1 = \partial_t, \quad X_2 = \partial_T \text{ (time translation and temperature shift)}$$

and infinite-dimensional sub-algebras

$$X_\pi = \pi(t)\,\partial_P \text{ (pressure shifts)}, \tag{3.5}$$

and transformation into an arbitrary rectilinearly moving coordinate system

$$X_{\chi i} = \chi_i(t)\partial_{x_i} + \chi_i'(t)\partial_{v_i} - \chi_i''(t)x_i\partial_P, \quad i = 1, 2, 3.$$

The translation and shift operators X_1, X_2 and X_π coincide with appropriate operators of the system (3.4). The turbulent model (3.4) conserves generalized Galilean invariance (2.5). It is important to note that the set of generators (3.5) does not contain the rotation-group generator of type X_8 as in (2.3). In simpler (k–ε)-models the group of rotations reflecting the property of space isotropy is also lost. This feature was corrected in the next generation of turbulent models of (k–ε) type. One of the examples is given below.

The governing equations for the averaged values of this model are [8]

$$\begin{aligned}
&\frac{\partial v_i}{\partial t} + v_\alpha \frac{\partial v_i}{\partial x_\alpha} + \frac{\partial P}{\partial x_i} = \nu \Delta v_i + \frac{\partial}{\partial x_\alpha}\left[\nu_t\left(\frac{\partial v_i}{\partial x_\alpha} + \frac{\partial v_\alpha}{\partial x_i}\right) - \frac{2}{3}\delta_{i\alpha}k\right], \quad \frac{\partial v_\alpha}{\partial x_\alpha} = 0,\\
&\frac{\partial k}{\partial t} + v_\alpha \frac{\partial k}{\partial x_\alpha} = \frac{\partial}{\partial x_\alpha}\left[(\nu + \nu_t)\frac{\partial k}{\partial x_\alpha}\right] + \left[\nu_t\left(\frac{\partial v_i}{\partial x_j} + \frac{\partial v_j}{\partial x_i}\right) - \frac{2}{3}\delta_{ij}k\right]\frac{\partial v_i}{\partial x_j},\\
&\frac{\partial \varepsilon}{\partial t} + v_\alpha \frac{\partial \varepsilon}{\partial x_\alpha} = \frac{\partial}{\partial x_\alpha}\left[\left(\nu + \frac{\nu_t}{\sigma_\varepsilon}\right)\frac{\partial \varepsilon}{\partial x_\alpha}\right] - c_{\varepsilon 1}\frac{\varepsilon}{e}\left[\nu_t\left(\frac{\partial v_i}{\partial x_j} + \frac{\partial v_j}{\partial x_i}\right) - \frac{2}{3}\delta_{ij}k\right]\frac{\partial v_i}{\partial x_j} + c_{\varepsilon 2}\frac{\varepsilon^2}{k},
\end{aligned} \tag{3.6}$$

where $c_\mu = 0{\cdot}09, c_{\varepsilon 1} = 1{\cdot}44, c_{\varepsilon 2} = 1{\cdot}92, \sigma_\varepsilon = 1{\cdot}3$.

The symmetry group of the system (3.6) with zero molecular viscosity $\nu = 0$ and $\sigma_\varepsilon \neq 1$ contains the generators

$X_1 = \partial_t$ (time translation),

$X_2 = 2t\partial_t + \mathbf{r}\partial_{\mathbf{r}} - \mathbf{v}\partial_{\mathbf{v}} - 2P\partial_P - 4\varepsilon\partial_\varepsilon - 2k\partial_k$ (expansions),

$X_{3-5} = x_i\partial_{x_j} - x_j\partial_{x_i} + v_i\partial_{v_j} - v_j\partial_{v_i}$, where $i = 1, 2, 3$ (rotations),

and infinite dimensional sub-algebras

$X_\pi = \pi(t)\partial_P$ (pressure shifts),

$X_{\chi i} = \chi_i(t)\partial_{x_i} + \chi_i'(t)\,\partial_{u_i} - \chi_i''(t)x_i\partial_P$ (generalized Galilean principle),

reflecting the basic properties of physical space and mechanical systems. The set of generators is equivalent to the set of Navier–Stokes equations.

In general, for complete evaluation of the reducibility of different sets of governing equations, in addition to comparison of point symmetries, it is necessary to search and analyze discrete symmetries and nonlocal symmetries. Traditionally, the great advantage of searching continuous symmetry groups is the existence of explicit computational methods in contrast to the procedure of searching the discrete symmetries. The new constructive method for searching discrete symmetries of differential equations based on the unification of continuous-group-theory methods, and on embedding the equations into the expanded cotangent space and on the technique of differential forms was developed [9, 10] and briefly presented below together with illustrative examples [11].

4. Discrete symmetries of governing equations

The regular method of searching discrete symmetries is based on the unification of continuous-groups analysis, embedding the problem into expanded cotangent space and differential-form techniques. Conditions of automorphism of applied transformations are used to direct the calculation of discrete symmetries.

In the general case the set of differential equations of common type,

$$Eq_k\left(\left\{x_j\right\},\left\{F_i\right\},\left\{F_i'\right\},\ldots,\left\{F_i^{(l)}\right\}\right)=0, \tag{4.1}$$

is considered, where $\left\{x_j\right\}$ and $\left\{F_i\right\}$ are sets of differential and field variables; consequently, $\left\{F_i'\right\},\left\{F_i''\right\},\ldots,\left\{F_i^{(l)}\right\}$ are the sets of all possible partial derivatives.

Under the action of a discrete transformation, using the formal procedure of the change of variables

$$\left(\left\{x_j\right\},\left\{F_i\right\}\right)\mapsto\left(\left\{\widetilde{x}_j,\left(x_j,F_i\right)\right\},\left\{\widetilde{F}_i\left(x_j,F_i\right)\right\}\right),$$

the system (4.1) is transformed into the form

$$\widetilde{E}_{q_k}\left(\left\{\widetilde{x}_j\right\},\left\{\tilde{F}_i\right\},\left\{\widetilde{F}_i'\right\},\left\{\widetilde{F}_i''\right\},\ldots,\left\{\widetilde{F}_i^{(n)}\right\}\right)=0 \tag{4.2}$$

System (4.1) can be presented by means of a differential-forms formalism on the basis of 1-form sets $\mathrm{d}x_1,\mathrm{d}x_2,\ldots,\mathrm{d}x_n,\mathrm{d}F_1,\mathrm{d}F_2,\ldots,\mathrm{d}F_m$ and $\mathrm{d}p^{(l)}_{q,ijk\ldots}$, where

$$\mathrm{d}p^{(l)}_{q,ijk\ldots}=\partial^{(l)}F_q/\partial x_i\partial x_j\partial x_k\ldots$$

designates the lth-order derivative of the qth field variable with respect to the differential variables $x_i,x_j,\ldots$ The indices $i,j,\ldots$ are arranged in a non-decreasing order. Consequently, system (4.2) has its own 1-form set $\mathrm{d}\widetilde{x}_1,\mathrm{d}\tilde{x}_2,\ldots\mathrm{d}\widetilde{x}_n,\mathrm{d}\widetilde{F}_1,\mathrm{d}\widetilde{F}_2,\ldots,\mathrm{d}\widetilde{F}_m$ and set $\mathrm{d}\widetilde{p}^{(l)}_{q,ijk}$.

The extended space $\mathrm{d}x_1,\ldots,\mathrm{d}\tilde{x}_1,\ldots$ is not a direct sum of its subspaces $\mathrm{d}x_1,\ldots,\mathrm{d}\tilde{x}_1,\ldots$ because the basic forms $\mathrm{d}x_1,\ldots,\mathrm{d}F_m$ and $\mathrm{d}\tilde{x}_1,\ldots,\mathrm{d}\tilde{F}_m$ are connected by the automorphism

$$L_{\mathbf{v}_l}\left(\mathrm{d}\tilde{x}_j\right)=b_l^k\widetilde{L}_{\mathbf{v}_l}(\mathrm{d}\tilde{x}_j),\quad L_{\mathbf{v}_l}\left(\mathrm{d}\widetilde{F}_i\right)=b_l^k\widetilde{L}_{\mathbf{v}_l}\left(\mathrm{d}\widetilde{F}_i\right), \tag{4.3}$$

where $L_{\mathbf{v}_l}()$, are Lie-generators for systems (4.1) and (4.2) acting in the spaces of the old and new coordinates, b_l^k are the constant coefficients of the nondegenerate automorphism matrix, and $\mathbf{v}_l$ is an infinitesimal symmetry isovector of (4.1).

The presence of automorphism (4.3) leads to the existence of diffeomorphism between derivatives of the field functions in the old $p^{(l)}_{q,ijk\ldots}$ and in the new $\widetilde{p}^{(l)}_{q,ijk\ldots}$ variables. The explicit representation of this diffeomorphism has the form of a nonlinear algebraic equations set.

In extended cotangent space two classes of 1-form are distinguished. The first one is a class of basic (or identically annulled) 1-forms and the second is a class of 1-forms annulled on the solutions of (4.1) and (4.2). The basic 1-forms are constructed in the form

$$\omega_i^{(b)}=\mathrm{d}F_i-\frac{\partial F_i}{\partial x_1}\mathrm{d}x_1-\frac{\partial F_i}{\partial x_2}\mathrm{d}x_2-\cdots-\frac{\partial F_i}{\partial x_n}\mathrm{d}x_n$$

In a similar manner, the 1-forms $\tilde{\omega}_i^{(b)}$ defined in a new coordinate space $\tilde{F}_i,\tilde{x}_j$ are constructed.

The differential forms annulled on solutions of (3.1) are obtained as

$$\omega_i^{(s)}=\sum A^{q,ijk\ldots}_{(l)}\mathrm{d}p^{(l)}_{q,ijk\ldots}+\sum B^j\mathrm{d}x_j.$$

A linear combination of functions $A^{1,ijk\ldots}_{(l)}$, B^j and their external product with appropriate forms of differential variables $\mathrm{d}x_i$ must be used to construct the set (4.1). An analogous procedure is used for constructing forms annulled on (4.2).

Let symmetry transformations be defined by the functions

$$\tilde{x}_k = \Phi_k\left(\{x_i\}, \left\{F_j\right\}\right), \quad \tilde{F}_l = \Psi_l\left(\{x_i\}, \left\{F_j\right\}\right). \tag{4.4}$$

The basic forms in new coordinates can be represented by the following relation using expressions (4.4), and the summation is assumed with respect to repeated indices

$$\tilde{\omega}_i^{(b)} = \mathrm{d}x_k\left(\frac{\partial}{\partial x_k} + \tilde{p}_{m,k}^{(1)}\frac{\partial}{\partial F_m}\right)\left(\Psi_i + \tilde{p}_{i,n}^{(1)}\Phi_n\right) = \Omega_i^k \mathrm{d}x_k, \qquad \text{where } \Omega_k^i = \left\langle \partial_{x_k} \middle| \tilde{\omega}_i^{(b)} \right\rangle. \tag{4.5}$$

In accordance with the definition and construction principle the obtained forms are the basic annulled forms. At the same time, the expansion (4.5) with respect to differential variable forms permits to treat the fact of annulling $\tilde{\omega}_i^{(b)}$ as a result of annulling all the components Ω_i^k and a system of connections defined in the extended space $\left\{p_{i,j}^{(1)}, \tilde{p}_{i,j}^{(1)}\right\}$ arises:

$$\Omega_i^k = 0, \quad i = 1, \ldots, m, \quad k = 1, \ldots, n \tag{4.6}$$

We define the existence of discrete symmetries as a closure condition of the basic annulled 1-forms (4.5) on the solutions of the extended set of equations. The analytic representation of this fact and the core of the method for searching the discrete symmetries have a form

$$\mathrm{d}\Omega_i^k = \lambda_i^{k,j}\omega_j^{(b)} + \mu_i^{k,p}\omega_p^{(s)} + \nu_i^{k,q}\omega_q^{(s)}, \tag{4.7}$$

where the summation is assumed with respect to repeated indices.

As a result of automorphism, (4.3), the forms $\left\{\tilde{\omega}_i^{(b)}\right\}$ do not appear in the linear combination (4.7). The given method does not need to solve first the difficult problem of searching for an infinitesimal symmetry isovector $\mathbf{v}_1$ of (4.1) [9]. On the other hand, the form $\tilde{\omega}_i^{(b)}$ is a vector in the cotangent space with components Ω_i^k. So the condition of the existence of discrete symmetries is reduced to the condition of potentiality of this vector on the solutions of (4.1) and (4.2). An illustration of a practical application of this technique in fluid dynamics problems is given below regarding a Bénard-convection structure.

5. Cell patterns in Bénard convection

The method is applied to the problem of stationary free convection in a layer of a homogeneous liquid heated from below. The kinetic coefficients of the liquid are functions of temperature; the linearized equation of state $\rho = \rho_0(1 - T)$ is used. Under the Boussinesq approximation the governing equations describing stationary Bénard convection are

$$\begin{aligned} &(\mathbf{v}\nabla)\,\mathbf{v} = -\nabla p + \nu\Delta\mathbf{v} + \nu_T'\left(2\left(\nabla T\nabla\right)\mathbf{v} + \nabla T \times \nabla \times \mathbf{v}\right) - T\mathbf{g}, \\ &\nabla\mathbf{v} = \mathbf{v}\nabla T = \chi\,\Delta T + \chi_T'\nabla T\cdot\nabla T + H\delta\left(z\right), \end{aligned} \tag{5.1}$$

where $\mathbf{v}$ is a velocity, P is a pressure without a hydrostatic part, T is the dimensionless temperature normalized by the heat-expansion coefficient of liquid, $\mathbf{g}$ is the gravity acceleration, ν, χ are the kinematic viscosity and temperature-conductivity coefficient, respectively, a prime denotes a derivative with respect to temperature, the term $H\delta(z)$ describes a plane horizontal heat source of intensity H.

Applying to the set (5.1) the given algorithm for searching discrete symmetries, one can produce a governing system of equations. The part of its solution describing the discrete

symmetry is

$$\tilde{x} = c\,(x\cos\vartheta + y\sin\vartheta)\,, \quad \tilde{y} = c\,(-x\sin\vartheta + y\cos\vartheta)\,, \quad \tilde{z} = cz, \quad c = \pm 1,$$
$$\tilde{T} = AT + T_0, \quad A = \kappa'_T\tilde{\kappa}/\tilde{\kappa}'_{\tilde{T}}\kappa, \quad T_0 = \text{const}, \quad \tilde{P} = \frac{\tilde{\kappa}}{c\kappa}P - cT_0 g, \tag{5.2}$$
$$\tilde{u} = \frac{\tilde{\kappa}}{c\kappa}\,(\mathrm{u}\cos\vartheta + v\sin\vartheta)\,, \quad \tilde{v} = \frac{\tilde{\kappa}}{c\kappa}\,(-\mathrm{u}\sin\vartheta + v\cos\vartheta)\,, \quad \tilde{w} = \frac{\tilde{\kappa}}{c\kappa}w,$$

where $\tilde{\kappa}\tilde{\kappa}'_{\tilde{T}} = c\kappa\tilde{\kappa}'_T$. In (5.2) κ is replaced by χ when the effect of the advective mechanism is disregarded or by ν in the other case, (x, y, z) is a Cartesian coordinate frame, u, v, w are corresponding velocity components; new variables are denoted by tildes. Under the action of (5.2), in accordance with (4.6), the tangent variables are transformed as follows:

$$\tilde{p}^{\tilde{x}}\cos\vartheta - \tilde{p}^{\tilde{y}}\sin\vartheta = \frac{\tilde{\kappa}^2}{c\kappa^2}p^x, \quad \tilde{p}^{\tilde{x}}\sin\vartheta + \tilde{p}^{\tilde{y}}\cos\vartheta = \frac{\tilde{\kappa}^2}{c\kappa^2}p^y, \quad \tilde{p}^{\tilde{z}} = \frac{\tilde{\kappa}^2}{c\kappa^2}p^z. \tag{5.3}$$

The value of angle ϑ remains to be defined. Let us consider the result of an n-fold action of (5.2) and (5.3) which is an identical transformation to any differential or field variable of (5.1). This condition defines the rotation angle

$$\vartheta = \frac{\pi}{2n}\left(3 - (-1)^n\right), \quad \text{if } c = 1, \quad \text{and} \quad \vartheta = \frac{2\pi}{n}, \quad \text{if } c = -1. \tag{5.4}$$

When $c = 1$ (the case of constant kinetic coefficients), the symmetry of the velocity field is defined by the rotational group $SO_n(2)$ when $n \neq 2^m$, or $SO_{2n}(2), n = 2^m$. If all convective cells belong to a unique symmetry group, the regular planar structure consists of one characteristic element. Such flows can be observed when $n = 2, 3, 6$, which corresponds to the rotational groups $SO_4(2)$ (squares), $SO_3(2)$ (triangles) and $SO_6(2)$ (hexagons). Such patterns are observed in both kinds of liquid. The results of the experiment (photos) [12] and theoretical analysis (schemes) are presented below in Figures 1–3.

The obtained structures can arise when all cells belong to subgroups of a common symmetry group. It is possible when $n = 4,\ 6$ with corresponding rotational groups $SO_8(2), SO_6(2)$. For the case of $SO_8(2)$ symmetry, the planar convective structure consists of regular (subgroup $SO_8(2)$) or irregular (subgroup $SO_4(2)$) octagons and squares (subgroup $SO_4(2)$).

Under degeneration of $SO_8(2)$ symmetry, when only the subgroup $SO_4(2)$ plays a role, the flow can be constructed on the basis of rectangular cells. For $SO_6(2)$ symmetry it is possible to form a cell pattern consisting of regular (subgroup $SO_6(2)$) and irregular (subgroup $SO_3(2)$) hexagons. These patterns can be formed only in liquid with temperature-dependent kinetic coefficients. Two-element systems are shown in Figures 4–5.

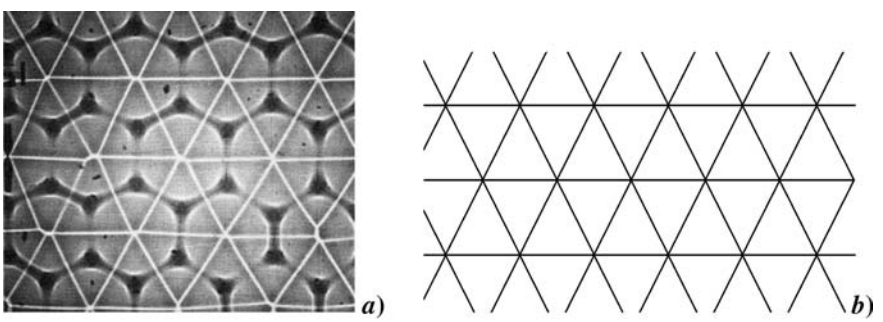

Figure 1. Regular triangles in convective flow structure: **a, b**) – experiments [12] and theory.

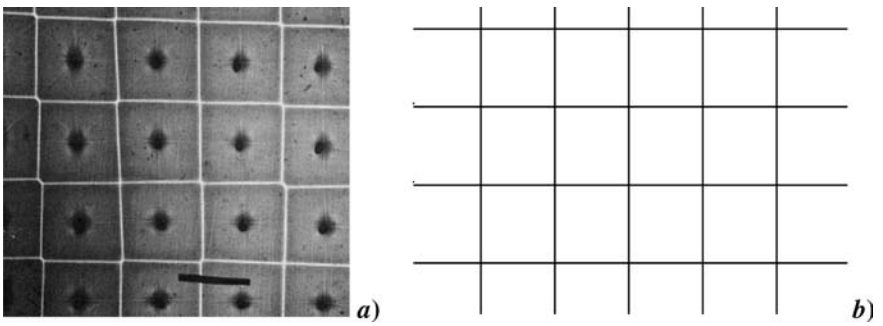

Figure 2. Regular squares in convective flow structure: **a, b**) – experiments [12] and theory.

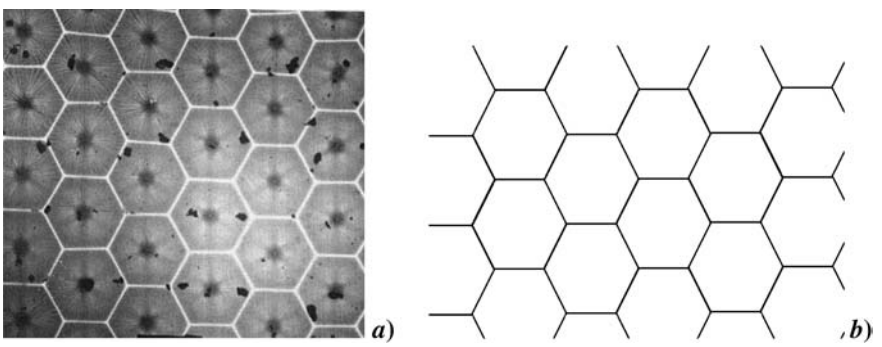

Figure 3. Regular hexagons in convective flow structure: **a, b**) – experiments [12] and theory.

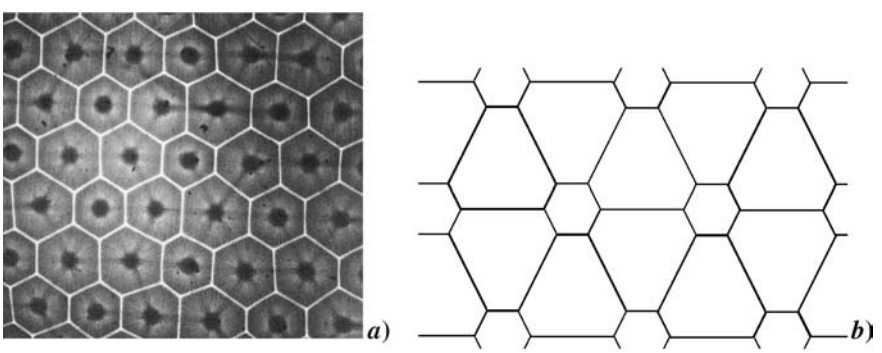

Figure 4. Regular and irregular hexagons in convective flow structure: **a, b**) – experiments [12] and theory.

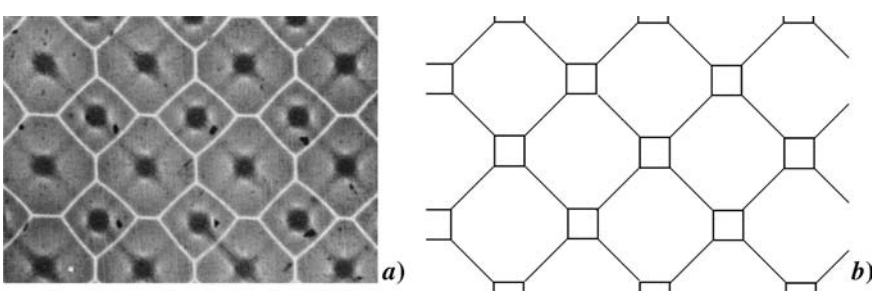

Figure 5. Regular squares and irregular octagons in convective flow structure: **a, b**) – experiments [12] and theory.

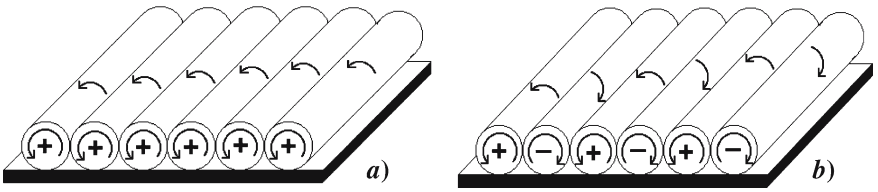

Figure 6. Roll regime of convection: **a)** – constant viscosity, **b)** – temperature-dependent viscosity.

In media with constant kinetic coefficients, the symmetry $SO_2(2)$ with discrete rotation angle π is absent. In the regime of roll convection, when all convective cells are horizontal cylinders, this means the exclusion of vorticity alternation in neighboring cells. Vorticity of 2D convective rolls has the same sign if the kinetic coefficients are constant, as is shown in Figure 6.

Alternative rotations in neighboring rolls occur in the general case but are unstable. All calculated regular forms have been observed in experiments [12].

For the case of temperature-dependent kinetic coefficients ($c=-1$) all above-described planar patterns are available, including $SO_2(2)$ symmetry. Corresponding structures are observed experimentally in a liquid with strong dependence of kinematic viscosity on temperature [12]. At the same time, the convective rolls of unique direction of rotation are longitudinally unstable and tend to transform into rectangular and square cells.

The direction of the flow in the center of the cell depends on the sign of the derivative of the kinetic coefficients on the temperature. If the kinetic coefficients are temperature-dependent, a change of the flow-circulation sign in cells is possible under the condition

$$\kappa\kappa'_T\big|_{T=T_1} = -\,\tilde{\kappa}\tilde{\kappa}'_T\big|_{T=T_2} \tag{5.5}$$

where κ is either the kinematic viscosity ν or the temperature-diffusivity coefficient χ. The illustration of this effect is presented below in the Figure 7. Such an effect has also been observed in experiments [13].

As follows from (5.2), a similar effect can be observed in a liquid with weakly varying kinematic-viscosity coefficient and strong dependence of the temperature-conductivity

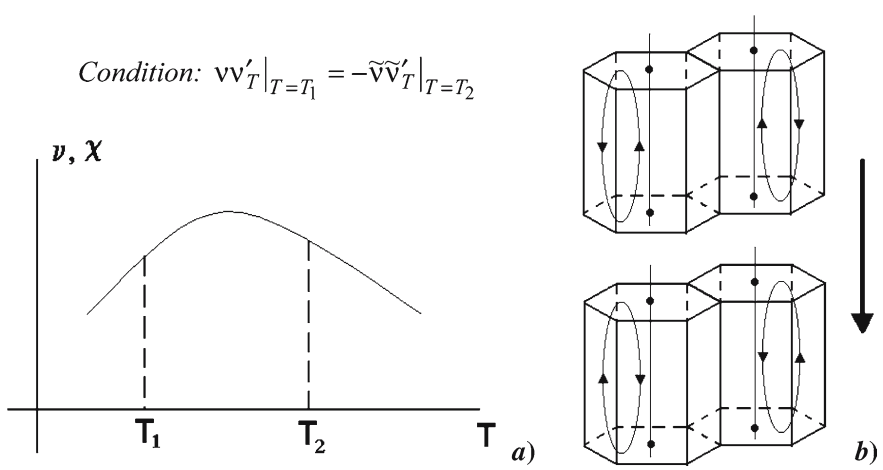

Figure 7. The change of velocity direction in cells due to variation of viscosity and temperature conductivities derivatives signs: **a)** – dependence of kinetic coefficients on temperature, **b)** – scheme of flow in the cells.

coefficient on temperature. Independently of the kind of convection pattern, all types of cells should be members of the unique symmetry group (or members of its subgroups) characterizing the observed phenomenon. The choice of the type of symmetry is defined by the physical parameters of the system and can be found by studying the temporal evolution of the system with real boundary conditions.

One of the important questions is the nature of thin interfaces and sharp boundaries between convective cells and the physics of their formation. Is this phenomenon typical for nonlinear models or can it be described in a linear approximation? To answer this question, a classification of periodic fluid motions is presented.

6. Classification of periodic motions of fluid

Each of the physical factors such as rotation, stratification, and compressibility of a fluid described by the set of governing equations (1.1) is associated with a characteristic type of wave flows, which are usually analyzed independently. When studying waves, dissipation effects are considered as corrections providing flow attenuation [1, 3]. However, in continua, dissipation factors determine the order of the equations and the total number of elements of periodic flows, including waves and sets of boundary layers on solid and free surfaces. Maintaining the order of the system of governing equations defined by the dissipation parameters enables one to find self-consistent solutions of linearized problems for the generation of internal waves described by Equations (2.1)–(2.2) without additional empirical parameters (force and mass sources [3]). In this connection the complete mathematical classification of three-dimensional periodic flows in the bulk of a fluid is given below, taking into account compressibility, stratification, rotation, and viscous-dissipation effects [14]. Diffusion and heat conduction are disregarded.

The linearized form of the set (2.1), taking into account compressibility of the medium, is analyzed. Oscillations of compressible stratified media are characterized by the buoyancy frequency $N=\sqrt{g/\Lambda}$ and adiabatic frequency $N_c=\sqrt{N^2-\frac{g^2}{c^2}}$, respectively, where c is the speed of sound.

We use the Cartesian coordinate system (x, y, z), where the z-axis is directed towards the zenith and the x- and y-axes are taken so that the corresponding projections of the angular velocity are equal to each other. In the linear approximation, the system of the equations of motion has the form

$$
\begin{aligned}
&\frac{\partial u}{\partial t}=-\frac{\partial P}{\partial x}+2\Omega\left(v\sin\varphi-\frac{1}{\sqrt{2}}w\cos\varphi\right)+\nu\Delta u+\left(\mu+\frac{\nu}{3}\right)\frac{\partial}{\partial x}\nabla\cdot\mathbf{v},\\
&\frac{\partial v}{\partial t}=-\frac{\partial P}{\partial y}+2\Omega\left(\frac{1}{\sqrt{2}}w\cos\varphi-u\sin\varphi\right)+\nu\Delta v+\left(\mu+\frac{\nu}{3}\right)\frac{\partial}{\partial y}\nabla\cdot\mathbf{v},\\
&\frac{\partial w}{\partial t}=-\frac{\partial P}{\partial z}+\sqrt{2}\Omega\ (u-v)\ \cos\varphi+\nu\Delta w+\left(\mu+\frac{\nu}{3}\right)\frac{\partial}{\partial z}\nabla\cdot\mathbf{v}-\rho g,\\
&\frac{\partial\rho}{\partial t}-\frac{w}{\Lambda}+\nabla\cdot\mathbf{v}=0,\quad \frac{\partial P}{\partial t}=-wg-c^2\nabla\cdot\mathbf{v}
\end{aligned}
\tag{6.1}
$$

where $\mathbf{v}=(u, v, w)$ is the velocity, P and ρ are the pressure minus hydrostatic pressure and medium-density perturbation normalized with respect to the density at the reference level $z=0$; φ is the latitude of the observation point, and ν and μ are the first and second kinematic viscosities.

System (1) is supplemented by the no-slip boundary conditions on rigid surfaces and the condition of damping of perturbations at infinity. The dynamic and kinematic boundary conditions on the free surface $z_s = \zeta(x, y)$ are [1]

$$(P - P_0)n_i - \left(\sigma'_{ik} - \sigma'^{(0)}_{ik}\right) n_k + \alpha n_i \Delta_\perp \zeta \Big|_{z=\zeta} = 0, \quad \partial\zeta / \partial t - w\big|_{z=\zeta} = 0, \tag{6.2}$$

where $\Delta_\perp = \partial^2/\partial x^2 + \partial^2/\partial y^2$, P and P_0 are pressures inside and outside the medium under consideration, respectively; σ'_{ik} and $\sigma'^{(0)}_{ik}$ are the corresponding viscous-stress tensors; α is the surface-tension coefficient; and n_i is the component of the unit normal to the surface. The analysis of system (1) is simplified when the viscosity coefficient and the ratio of the media in contact (*e.g.*, liquid and gas) is small.

When studying periodic flows $\mathbf{v} = \mathbf{v}_0 \exp(\mathrm{i}\mathbf{kr} - \mathrm{i}\omega t)$, $P = P_0 \exp(\mathrm{i}\mathbf{kr} - \mathrm{i}\omega t)$, $\rho = \rho_0 \exp(\mathrm{i}\mathbf{kr} - i\omega t)$ with frequency ω and wave vector $\mathbf{k} = (k_x, k_y, k_z)$, the general solution of the system (1) can be written as a superposition of elementary waves

$$A = \sum_j \int_{-\infty}^{+\infty}\int_{-\infty}^{+\infty} a_j\,(k_x, k_y) \exp\left(\mathrm{i}\,\left(k_{zj}\,(k_x, k_y)\, z + k_x x + k_y y - \omega t\right)\right) \mathrm{d}k_x\,\mathrm{d}k_y, \tag{6.3}$$

where A is a velocity component, pressure, or density. The summation must be performed over all roots of the dispersion equation that are obtained when the solution of (6.1) is substituted in the boundary conditions of the problem or in the radiation condition in an unbounded medium (attenuation of perturbations at infinity).

For stationary periodic waves, the frequency ω is fixed, and the dispersion equation describes the relation between the wavenumber components that is expressed as $k_{zj}(k_x, k_y)$ for given k_x and k_y values. The solution of the dispersion relation contains two types of roots. Regular on viscosity roots, ($\Im\mathrm{m}\, k_{zj}\,(k_x, k_y) \sim \nu^\alpha$, where α is positive number), which have their analogues in ideal fluids ($\nu \to 0, \Im\mathrm{m}\, k_{zj} \to 0$), describe waves. Singular on viscosity roots ($\Im\mathrm{m}\, k_{zj} \sim \nu^{-\alpha}$) describe boundary layers. The power of the dispersive equation defines the number of singular roots and consequently the number of types of boundary layer. The open question is what elements of flow can propagate in the fluid body? Are they only waves or waves and analogues of boundary layers, which look like singular interfaces in a fluid interior? Singular interfaces are observed inside a lee-waves field past an obstacle in a continuously stratified fluid [15].

Generally speaking, the system (6.1) with boundary conditions (6.2) admits two types of waves that are surface waves whose amplitude decreases monotonically with the distance from the boundary and internal waves with maximum displacements in the bulk of the fluid. When the media in contact have considerably different densities, their properties can be analyzed independently [1].

For flows in the bulk of the fluid, the substitution of (6.3) in (6.1) yields a system of algebraic equations for the amplitudes $u_0, v_0, w_0, P_0, \rho_0$

$$\begin{aligned}
&\left(\mathrm{i}\omega - \nu k^2 - (\mu + \nu/3)\, k_x^2\right) \mathrm{u}_0 + \left(2\Omega \sin\varphi - (\mu + \nu/3)\, k_x\, k_y\right) v_0 - \\
&\quad - \left(\sqrt{2}\Omega \cos\varphi + (\mu + \nu/3)\, k_x\, k_z\right) w_0 - \mathrm{i}k_x P_0 = 0, \\
&- \left(2\Omega \sin\varphi + (\mu + \nu/3)\, k_x k_y\right) u_0 + \left(\mathrm{i}\omega - \nu k^2 - (\mu + \nu/3)\, k_y^2\right) v_0 + \\
&\quad + \left(\sqrt{2}\Omega \cos\varphi - (\mu + \nu/3)\, k_y\, k_z\right) w_0 - \mathrm{i}k_y P_0 = 0,
\end{aligned} \tag{6.4}$$

$$\left(\sqrt{2}\Omega\cos\varphi-\left(\mu+\nu/3\right)k_x k_z\right)u_0-\left(\sqrt{2}\Omega\cos\varphi+\left(\mu+\nu/3\right)k_y k_z\right)v_0+$$
$$+\left(\mathrm{i}\omega-\nu k^2-\left(\mu+\nu/3\right)k_z^2\right)w_0-\mathrm{i}k_z P_0-g\rho_0=0,$$
$$-\mathrm{i}k_x u_0-\mathrm{i}k_y v_0+\left(1/\Lambda-\mathrm{i}k_z\right)w_0+\mathrm{i}\omega\rho_0=0,$$
$$-\mathrm{i}k_x c^2 u_0-\mathrm{i}k_y c^2 v_0+\left(g-\mathrm{i}k_z c^2\right)w_0+\mathrm{i}\omega P_0=0,$$

where $k^2=k_x^2+k_y^2+k_z^2$.

From the condition of the existence of a nontrivial solution, a dispersion equation for hybrid 3D waves of the most general type follows:

$$\omega D_\nu(k)\left(\omega D_\nu(k)\tilde{D}_\nu(k)+2\sqrt{2}\omega\Omega g\left(k_y-k_x\right)\cos\varphi\right)-$$
$$-\omega D_\nu(k)N^2\left(D_\nu(k)+\mathrm{i}\left(\mu+\nu/3\right)k_\perp^2\right)+$$
$$+4\omega\Omega^2\left(N^2\sin^2\varphi-\omega\left(D_\nu(k)+\mathrm{i}\left(\mu+\nu/3\right)f^2(k)\right)\right)+$$
$$+c^2\left(D_\nu(k)\left(N_c^2k_\perp^2-\omega k^2D_\nu(k)\right)+4\omega\Omega^2 f^2(k)\right)=0, \tag{6.5}$$

where $f(k)=k_z\sin\varphi+\left(k_x+k_y\right)\cos\varphi/\sqrt{2}$, $\tilde{D}_\nu(k)=\omega+\mathrm{i}\left(4\nu/3+\mu\right)k^2$, $D_\nu(k)=\omega+\mathrm{i}\nu k^2$.

Dispersion Equation (6.5) for the wavenumber k is singularly perturbed, because the leading, k^6, term involves a small factor ν^2. In the general case, two of the six roots of (6.5) are regular in viscosity and describe the propagation of wave perturbations and the remaining four roots characterize the set of coexisting boundary layers. Single-frequency boundary layers differ from each other in thickness and other properties. Their number and behavior generally depend on the space dimension and are determined by the boundary conditions.

Solutions of (6.5) are further analyzed in the spherical coordinate system (k,Ψ,Θ) introduced in the wavenumber space $\left(k_x,k_y,k_z\right)$ by the relations $k_x=k\sin\Theta\cos\Psi$, $k_y=k\sin\Theta\sin\Psi$, $k_z=k\cos\Theta$. In this analysis, both types of singular solutions, as well as solutions that are regular in viscosity, are preserved.

The domain of existence of propagating waves that have real frequency ω and are characterized by dispersion relation (6.5) depends on many factors, such as the wave ratio and intrinsic rotation and buoyancy frequencies, the compressibility of the medium, and the geometry of the problem, and is determined by the inequality

$$2\omega^2\Omega^2\sin^2\Theta\cos^2\varphi\left(\sin\Psi-\cos\Psi\right)^2\geq\frac{c^2\left(4\Omega^2\left(N^2\sin^2\varphi-\omega^2\right)-\omega^2\left(N^2-\omega^2\right)\right)}{g^2\left(N_c^2\sin^2\Theta-\omega^2+4\Omega^2F^2\right)}, \tag{6.6}$$

which is simplified for certain types of waves.

In an unbounded medium, on a plane to which the normal is characterized by angles Ψ and Θ, there are two boundary layers with thicknesses

$$\delta_{b\pm}=\sqrt{\frac{2\nu}{|\omega_\pm-\omega|}},\quad \omega_\pm=\frac{N_c^2}{2\omega}\sin^2\Theta\left[1\pm\sqrt{1+\frac{16\omega^2\Omega^2F^2}{N_c^4\sin^4\Theta}}\right], \tag{6.7}$$

where $F=\left(\sqrt{2}\cos\Theta\sin\varphi+\sin\Theta\left(\sin\Psi+\cos\Psi\right)\cos\varphi\right)/\sqrt{2}$.

These boundary layers exist together with three-dimensional waves. Since the condition $g\Lambda/c^2\ll1$ is satisfied for virtually all media, the adiabatic frequency N_c in the expressions for $\omega_\pm$ in (6.7) can be approximately replaced by the buoyancy frequency N.

Taking into account compressibility and disregarding rotation effects ($\Omega=0$), we conclude from (6.5) that propagating three-dimensional acoustic gravity waves exist in two frequency

bands $\omega \le N_c$ and $\omega \ge N$. In the $\omega \ll N_c$ band, they exhibit the properties of internal gravity waves. Their properties for $\omega \gg N$ approach those of isotropic sound. Simultaneously with waves, two types of boundary layers with the characteristic thicknesses

$$\delta_{St} = \delta_N \sqrt{2/\sin\Theta_\omega}, \quad \delta_i = \delta_N \sqrt{\frac{2\sin\Theta_\omega}{\left|\left(1-\frac{g\Lambda}{c^2}\right)\sin^2\Theta - \sin^2\Theta_\omega\right|}} \approx \delta_N \sqrt{\frac{2\sin\Theta_\omega}{\left|\sin^2\Theta - \sin^2\Theta_\omega\right|}}, \quad (6.8)$$

where $\delta_N = \sqrt{\nu/N}$, $\Theta_\omega = \arcsin(\omega/N)$, are formed at rigid boundaries. The first of them is similar to periodic Stokes flow in a homogeneous fluid [1], and the second, whose parameters depend both on the buoyancy frequency N and on the speed of sound c, is specific for stratified media. The universal microscale $\delta_N = \sqrt{\nu/N}$ is common for both boundary layers. The thicknesses of the boundary layers also depend on the slopes of the waves and bounding surfaces.

The frequency band $\omega_- < \omega < \omega_+$ of the existence of inertial gravity waves in stratified rotating incompressible media is limited by the values

$$\omega_\pm^2 = \frac{1}{2}\left(N^2 + 4\Omega^2 \pm \sqrt{\left(N^2 + 4\Omega^2\cos 2\varphi\right)^2 + 16\Omega^4 \sin^2 2\varphi}\right),$$

which depend on the latitude of the observation point. Simultaneously with 3D inertial gravity waves, there are two types of boundary layers with the scales

$$\delta_{b\pm} = \delta_N \sqrt{\frac{2}{|\omega_\pm - \omega^*|}}, \quad \omega_\pm = \frac{\sin^2\Theta}{2\omega^*}\left[1 \pm \sqrt{1 + \frac{16\omega^2\Omega^2F^2}{N^4\sin^4\Theta}}\right], \quad \omega^* = \frac{\omega}{N}. \quad (6.9)$$

Inertial acoustic waves in a homogeneous fluid ($N = 0$) coexist with two separated boundary layers with the thickness

$$\delta_{b\pm} = \sqrt{\frac{\nu}{\Omega\,|F \pm \cos\Theta_\omega|}}, \quad (6.10)$$

where $\Theta_\omega = \arccos(\omega/2\Omega)$ is the slope of the propagation lines of the inertial acoustic waves to the horizon. One of these waves with thickness δ_{b+} is an analogue of the well-known Ekman layer. Periodic flows have the properties of inertial and acoustic waves for $\omega \ll \Omega$ and the opposite case, respectively.

Three-dimensional acoustic waves in a homogeneous fluid ($N = \Omega = 0$) are characterized by the dispersion $\omega^2 = k^2\left(c^2 - \mathrm{i}\omega\left(4\nu/3 + \mu\right)\right)$. In this case two sets of boundary layers are joined in the united doubly degenerate Stokes layer with the thickness $\delta_b = \sqrt{2\nu/\omega}$. Perturbations within this layer are transverse with zero divergence of the velocity; *i.e.*, the fluid within it behaves as incompressible.

From the form of the dispersion of three-dimensional periodic perturbations in a homogeneous incompressible fluid, $k^2\left(\omega + \mathrm{i}\nu k^2\right)^2 = 0$, when $(N = \Omega = \nabla\cdot\mathbf{v} = 0)$, it follows that this medium is free of developed propagating waves. A doubly degenerate viscous boundary layer consisting of two periodic Stokes flows with thickness $\delta_b = \sqrt{2\nu/\omega}$ is formed on the rigid oscillating boundary. It means that classical 3D Navier–Stokes equations, both for compressible and incompressible fluids, form an ill-posed problem due to the merging of boundary layers. The degeneration of Navier–Stokes equations for homogeneous fluids is removed by additional symmetry posed by boundary conditions (2D problems, axial-symmetric problems).

The inclusion of thermal diffusivity and diffusion in multicomponent media leads to both the appearance of additional equations in the system (6.1) of the equations of motion and to the increasing of the order of the system and the number of types of boundary layers. Each dissipative factor gives room for the appearance of a new pair of boundary layers, which can be either completely or partially separated. Some simple examples of composed boundary layers are discussed in [16].

Large-scale wave and fine-structure boundary-layer elements are inseparable components of the united system of periodic flows. All elements of this system are formed and disappear simultaneously, regardless of differences in their spatial scales.

In the general case, the regular parts of periodic solutions for stratified rotating media are matched with solutions of similar problems in a stratified or homogeneous fluid at rest. In a homogeneous fluid two different boundary layers merge in the united degenerate layer. There are discontinuities on wave characteristics in a stratified ideal fluid [17]. Similar structures in the periodic wave-beams in a viscous fluid have not been recognized up to now. The inverse analytic extrapolation of solutions in an ideal fluid into a viscous fluid is impossible because of the insufficient completeness of the original functional space.

In the general case, the dynamics of hydrodynamic systems is determined by the nonlinear interaction between all structural elements of flows that are large-scale waves and thin boundary layers. For example, variation of the thicknes and nonlinear interaction of boundary layers can lead to generation in cases, when direct excitation of waves in linear theory is forbidden by the condition of infinitesimal-wave propagation [3, Chapter 4, pp. 375–385]. Nonlinear generation of periodic waves by boundary layers on a circular disk performing torsion (angular) oscillations has been studied theoretically and experimentally [18, 19]. Results are in reasonable agreement in the range of flow parameters where effects related to the formation of edge vortices are negligible. Generation of internal waves by interacting boundary layers is studied in [20].

Owing to large vorticity, interacting boundary layers are effective generators of vortex motions. Experimental studies of the dynamics of boundary layers and the generation of vortices require substantial improvement of instruments for visualization and flow measurement. These instruments must visualize the flow field and resolve the fine structure of the smallest elements in the flow.

An illustration of the practical use of the described approach to study periodic motions is presented below. The 3D generalization of the classical Stokes problem for continuously stratified fluid is discussed. We analyze the generation of fluid motions by a compact plane source oscillating in a sloping rigid plane. It is known that periodic motions of compact sources in a stratified field produce periodic boundary layer and internal waves. A more detailed analysis shows that a self-consistent solution satisfying exact boundary conditions describes, in addition to the wave cone, two different embedded boundary layers. Numerical visualization of the solutions shows that singular structures manifest themselves not only on an emitting surface but also at the edges of the wave cone.

7. Internal waves and internal boundary layers in a continuously stratified fluid

An exact calculation of 3D harmonic internal-waves generation has been carried out before only for a single special case, namely when the source is part of the surface of a vertical cylinder [21]. In this case the calculations are simplified considerably due to the matching between the symmetries of the radiator and the wave-field geometry.

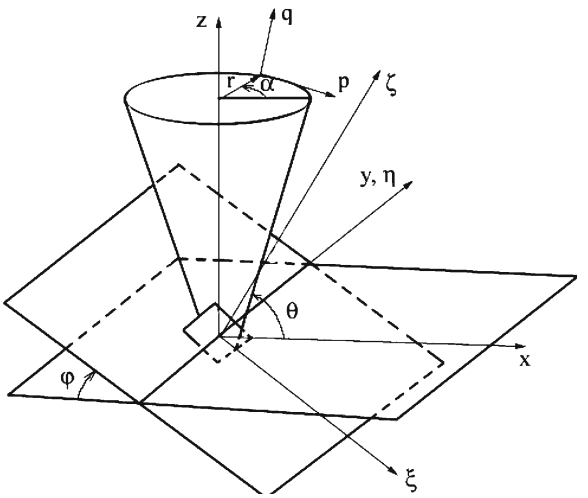

Figure 8. Coordinate frames.

When the source of a fluid motion is a rectangle or an ellipse oscillating along a rigid plane, the linearized system (2.1) for stratified fluid motions in the Boussinesq approximation (2.2) is

$$\rho_0 \frac{\partial \mathbf{v}}{\partial t} = -\nabla P + \rho_0 \nu \Delta \mathbf{v} - \rho g \mathbf{e}_z, \quad \frac{\partial \rho}{\partial t} + v_z \frac{\mathrm{d}\rho_0}{\mathrm{d}z} = 0, \quad \text{div } \mathbf{v} = 0, \tag{7.1}$$

where P, ρ and $\mathbf{v} = (v_x, v_y, v_z)$ are the pressure density and velocity of the fluid; ν is the kinematic viscosity, g is the acceleration due to gravity directed opposite to the axis Oz. Part of the surface makes oscillations with velocity $\mathbf{v}(\xi, \eta, t)$, where ξ, η are coordinates along a plane (Figure 8). The boundary conditions are no-slip for the velocity on the whole surface and attenuation of all disturbances at infinity.

To simplify the calculations we use four coordinate systems, which are shown in Figure 8. The line of action of the gravity force defines the reference to the laboratory coordinate system (x, y, z). The local coordinate system (ξ, η, ζ) is connected with the emitting surface, which lies in the $O\xi\eta$ plane and, without loss of generality, can be obtained by rotating the laboratory coordinate system (x, y, z) by an angle φ around the y-axis. With the wave cone connected, the attached system of coordinates is (q, p, α), where the q-axis is directed along the wave cone, the p-axis is directed transversely, and α is an angular variable. The following relations exist between these systems

$$\xi = x\cos\varphi + z\sin\varphi, \quad \eta = y, \quad \zeta = -x\sin\varphi + z\cos\varphi, \quad x = r\cos\alpha, \quad y = r\sin\alpha \quad z = z,$$
$$p = r\sin\theta - z\cos\theta, \quad q = r\cos\theta + z\sin\theta \tag{7.2}$$

We consider stationary periodical oscillations, when the time dependence of all quantities is $\exp(-\mathrm{i}\omega t)$ and the forcing frequency ω is the constant. This factor is omitted below.

In an incompressible fluid two auxiliary scalar functions Ψ, Φ, defining the velocity vector, are introduced to simplify the calculations (toroidal – poloidal decomposition [22])

$$\mathbf{v} = \nabla \times \mathbf{e}_z \Phi + \nabla \times (\nabla \times \mathbf{e}_z \Psi), \tag{7.3}$$

The system (7.1) is now transformed into two disconnected equations

$$\left(\omega^2 \Delta - N^2 \Delta_\perp - \mathrm{i}\omega\nu\Delta^2\right) \Delta_\perp \Phi = 0, \quad (\omega - \mathrm{i}\nu\,\Delta)\,\Delta_\perp \Psi = 0, \tag{7.4}$$

where $\Delta_\perp = \partial_x^2 + \partial_y^2$. Solutions the equations $\Delta_\perp \Phi, \Delta_\perp \Psi = 0$ describing isopycnic and non-dissipative motions are not realised in physical experiments. These equations are the result of the system of governing equations increasing when one uses a toroidal-poloidal decomposition [22] and are not analyzed below. A more detailed analysis of the physical properties of these operations is presented in [23]. Then Equation (7.4) is transformed into

$$\left(\omega^2 \Delta - N^2 \Delta_\perp - \mathrm{i}\omega\nu\Delta^2\right) \Phi = 0, \quad (\omega - \mathrm{i}\nu\Delta)\ \Psi = 0 \tag{7.5}$$

Solutions of (7.4) are constructed by an integral method using Fourier transforms

$$\Phi = \int_{-\infty}^{+\infty} \left[A(k_\xi, k_\eta) \mathrm{e}^{\mathrm{i}k_1\zeta} + B(k_\xi, k_\eta) \mathrm{e}^{\mathrm{i}k_2\zeta} \right] \mathrm{e}^{\mathrm{i}k_\xi\xi + \mathrm{i}k_\eta\eta} \mathrm{d}k_\xi \mathrm{d}k_\eta, \tag{7.6}$$

$$\Psi = \int_{-\infty}^{+\infty} C(k_\xi, k_\eta) \mathrm{e}^{\mathrm{i}k_3\zeta + \mathrm{i}k_\xi\xi + \mathrm{i}k_\eta\eta} \mathrm{d}k_\xi \mathrm{d}k_\eta, \quad \zeta > 0,$$

where components of wave vectors are defined by the solutions of the dispersion equation corresponding to the system (7.5) and are expressed in terms of two components of the wave vector $k_i(k_\xi, k_\eta)$, $i = 1, 2, 3$:

$$\left[\mathrm{i}\nu\left(k_3^2 + k_\perp^2\right) + \omega\right] \left\{\omega^2 \left(k^2 + k_\perp^2\right) - N^2 \left[\left(k_\xi \cos\varphi - k \sin\varphi\right)^2 + k_\eta^2\right] + \mathrm{i}\omega\nu \left(k^2 + k_\perp^2\right)^2\right\} = 0. \tag{7.7}$$

There is one solution of (7.6) which is regular with respect to the viscosity. It describes the propagation of internal wave beams with a wavelength $\lambda - 2\pi/k$ defined by the boundary conditions. There are two solutions that are singular with respect to the viscosity. These describe a boundary layer with characteristic thickness $\delta_N = \sqrt{\nu/N}$ [23]. The boundary layers reflect a balance between the inertial, buoyancy and viscous forces in the vicinity of the rigid surface.

The solutions of the dispersion equations (for small enough viscosity) can be found by standard perturbation methods

$$k_1 = k_1^{(0)} + \mathrm{i}\,\nu\, k_1^{(1)}; \quad k_1^{(0)} = \left(k_\xi \sin 2\varphi + 2\kappa \cos\theta\right)/2\mu,$$

$$k_1^{(1)} = \frac{\sin\theta\ \left(k_\xi \sin\varphi \cos\theta + \kappa \cos\varphi\right)^4}{2N\,\mu^4\,\kappa\cos\theta}, \quad k_2 = \frac{\mathrm{i} + \mathrm{sign}\mu}{\delta_\varphi} - \frac{k_\xi \sin 2\varphi}{2\mu}, \tag{7.8}$$

$$k_3 = \frac{\mathrm{i}+1}{\delta_\nu} + \frac{\mathrm{i}+1}{4}\delta_\nu \left(k_\xi^2 + k_\eta^2\right),$$

where $\theta = \arcsin(\omega/N)$ is the inclination of the internal wave-propagation direction to the horizontal, $\kappa = \sqrt{k_\xi^2 \sin^2\theta - \mu\, k_\eta^2}$, $\mu = \sin^2\varphi - \sin^2\theta$, $\delta_\nu = \sqrt{2\nu/\omega}$, $\delta_\varphi = \sqrt{2\nu \sin\theta / N\,|\mu|}$.

Only the imaginary part of the root k_1 differs from the wavenumber for waves in an ideal liquid. The real part defines propagating waves, and the imaginary part defines the spatial structure of the beam and viscous damping. Therefore, the member with a spectral density $A(k_\xi, k_\eta)$ describes internal waves. Roots k_2 and k_3 with a characteristic scale $O(\sqrt{\nu/\omega})$ have no counterpart in an ideal fluid and tend to infinity at $\nu \to 0$ and the expression with coefficient $B(k_\xi, k_\eta)$ corresponds to an internal boundary layer with thickness $\delta_\varphi = \sqrt{2\nu \sin\theta / N\,|\mu|} = \delta_N f(\theta, \varphi)$. This type of boundary layer is specific for a stratified fluid. And the coefficient $C(k_\xi, k_\eta)$ corresponds to a viscous-wave boundary layer with thickness $\delta_{St} = \sqrt{2\nu/\omega} = \delta_N f(\theta)$, existing both in viscous homogeneous, and in a stratified liquid. The roots k_2 and k_3 also describe boundary currents inside the wave-beam.

Substituting (7.6) in the boundary condition, we obtain a linear system defining the spectral coefficients A, B, C. The solution of the system is

$$\begin{pmatrix} A \\ B \\ C \end{pmatrix} = \frac{1}{\Delta} \begin{pmatrix} D_{11} & D_{12} & D_{31} \\ D_{21} & D_{22} & D_{32} \\ D_{31} & D_{32} & D_{33} \end{pmatrix} \cdot \begin{pmatrix} U_\xi \\ U_\eta \\ U_\zeta \end{pmatrix} \tag{7.9}$$

where the coefficients of the matrix $D_{i\,j}$ are

$$D_{11} = -\mathrm{i}k_\eta^2 \left[k_\xi + \frac{1}{2}(k_2 - k_3)\sin 2\varphi \right] - \mathrm{i}k_\xi \beta_2 \beta_3, \quad D_{12} = -\mathrm{i}k_\eta \left(k_\eta^2 + \beta_2^2 \right),$$

$$D_{13} = -\mathrm{i}k_\eta^2 \left[(k_2 - k_3)\cos^2\varphi + k_3 \right] - \mathrm{i}k_2 \beta_2 \beta_3, \quad D_{21} = -ik_\eta^2 \left[k_\xi + \frac{1}{2}(k_1 - k_3)\sin 2\varphi \right] - \mathrm{i}k_\xi \beta_1 \beta_3,$$

$$D_{22} = -\mathrm{i}k_\eta \left(k_\eta^2 + \beta_1^2 \right), \quad D_{23} = -\mathrm{i}k_\eta^2 \left[(k_1 - k_3)\cos^2\varphi + k_3 \right] + \mathrm{i}k_1 \beta_1 \beta_3,$$

$$D_{31} = \left(k_\eta^2 \cos^2\varphi + k_\xi^2 \right)(k_1 - k_2)\, k_\eta,$$

$$D_{32} = (k_1 - k_2) \left[-k_\xi \beta_1 \beta_2 + k_\eta^2 \left(\frac{1}{2}(k_1 + k_2)\sin 2\varphi + k_\xi \cos 2\varphi \right) \right],$$

$$D_{33} = (k_1 - k_2)\, k_\eta \sin\varphi \left[-k_\eta^2 \cos\varphi + k_\eta \left(k_1 \gamma_2 + k_\xi \beta_2 \right) \right],$$

$$\Delta = (k_1 - k_2) \left\{ -k_\xi \beta_1 \beta_2 \beta_3 + \mathrm{i}k_\eta^4 \cos\varphi + \mathrm{i}k_\eta^2 \left[\beta_3 \left(\gamma_1 \sin\varphi + \beta_2 \cos\varphi \right) + \gamma_1 \beta_1^2 - \gamma_2 \beta_2^2 \right] \right\}$$

Here $\mathbf{U} = \frac{1}{4\pi^2} \int_{-\infty}^{+\infty} \mathbf{v}(\xi, \eta) \mathrm{e}^{-\mathrm{i}k_\xi \xi - \mathrm{i}k_\eta \eta} \mathrm{d}\xi\, \mathrm{d}\eta$ is the Fourier transform of the velocity, and $\beta_i = k_i \sin\varphi - k_\xi \cos\varphi$, $\gamma_i = k_i \cos\varphi + k_\xi \sin\varphi$.

The expressions (7.6) are the general solution of the linearized periodic internal wave-generation problem satisfying the boundary conditions exactly, where the spectral coefficients $A(k_\xi, k_\eta)$, $B(k_\xi, k_\eta)$ and $C(k_\xi, k_\eta)$ are defined by expressions (7.9) and k_1, k_2, k_3 are defined by formulas (7.8).

The calculations are completed for two practically important generator shapes of that are used in experiments. We study disturbances produced by a rectangular and a circular disk in a fluid with low viscosity and weak stratification. Wave-field parameters are calculated at large distances from the source oscillating along the plane (shear source), transverse (piston source) and bi-transversal (bi-pistons). Conditions for the applicability of standard approximations valid for small ratios of the boundary-layer thicknesses and wavelength are defined. Results of wave attenuations along a central cone or centre plane for different 2D and 3D sources are presented in Table 3.

In limiting cases all constructed solutions are matched continuously to each other and with well-known exact solutions. The solutions are written in a form that allows easy comparison with laboratory experiments.

If the wave source is a horizontal disk of radius R, oscillating in a vertical direction with velocity amplitude U and frequency ω then the stream function of the propagating disturbances is calculated from (7.6):

$$\Psi = UR \int_0^\infty \frac{J_1(kr)}{k(k_2 - k_1)} \left[k_2 \mathrm{e}^{\mathrm{i}k_1(k)z} + k_1 \mathrm{e}^{\mathrm{i}k_2(k)z} \right] \mathrm{d}k \tag{7.10}$$

Table 3. Vertical displacements $h(0,q)$ along the central wave cone (wedge in 2D case) for different 2D and 3D small sources ($a, b \ll L_\nu, q \gg a, b, L_\nu = \sqrt[3]{g\nu}/N$).

Type of a source	Strip (2D)	Rectangular (3D)	Disk (3D)
Longitudinally moving surface (shear source)	$\frac{\lambda_0 a}{\delta_N^{1/3}} \frac{1}{q^{2/3}}$	$\frac{\lambda_0 ab}{\delta_N^{2/3}} \frac{1}{q^{4/3}}$	$\frac{\lambda_0 R^2}{\delta_N^{2/3}} \frac{1}{q^{4/3}}$
Transversally moving surface (piston source)	$\frac{\lambda_0 a}{\delta_N^{2/3}} \frac{1}{q^{1/3}}$	$\frac{\lambda_0 ab}{\delta_N} \frac{1}{q}$	$\frac{\lambda_0 R^2}{\delta_N} \frac{1}{q}$
Bi-piston moving surface	$\frac{\lambda_0 a}{\delta_N^{4/3}} \frac{a}{q^{2/3}}$	$\frac{\lambda_0 ab}{\delta_N^{5/3}} \frac{b}{q^{4/3}}$	–

$\delta_N = \sqrt{\nu/N}$ is universal microscale of periodic motions, $\lambda_0 = u_0/N$ – characteristic wavelength.

where the regular root (proportional ν) and the singular root $\left(\sim 1/\sqrt{\nu}\right)$ of the dispersion relations $\omega^2\left(k^2+k_{1,2}^2\right) - N^2k^2 + \mathrm{i}\nu\omega\left(k^2+k_{1,2}^2\right)^2 = 0$ are

$$k_1^2 = -k^2 + \frac{\mathrm{i}\sin\theta}{2\delta_N^2}\left[1 - \sqrt{1 + \frac{4\mathrm{i}k^2\delta_N^2}{\sin^3\theta}}\right], \quad k_2^2 = -k^2 + \frac{\mathrm{i}\sin\theta}{2\delta_N^2}\left[1 + \sqrt{1 + \frac{4\mathrm{i}k^2\delta_N^2}{\sin^3\theta}}\right], \tag{7.11}$$

where $\delta_N = \sqrt{\nu/N}, \theta = \arcsin(\omega/N)$ is the slope of the wave cone to the horizon. Wavenumber k_1 corresponds to propagating waves, wavenumber k_2 describes the boundary layer with lengthscale $\delta_\omega = \delta_N\sqrt{2/\sin\theta}$. The condition of attenuation of all disturbances in the upper half-plane ($z \geq 0$) at infinity is satisfied at the next values of the roots $\Im\mathrm{m}\, k_1 > 0$ and $\Im\mathrm{m}\, k_2 > 0$. The spatial structure of the wave cone is defined by the imaginary part of the solution (7.10), which is not small, even in the case of weak stratification and small viscosity.

From (7.10) the next expressions for the vertical and radial components of the velocity are as follows:

$$v_z = UR\int_0^{+\infty} \frac{J_1(kR)\,J_0(kr)}{k_2 - k_1}\left(k_2\mathrm{e}^{\mathrm{i}k_1 z} - k_1\mathrm{e}^{\mathrm{i}k_2 z}\right)\mathrm{d}k, \tag{7.12}$$

$$v_r = -\mathrm{i}UR\int_0^{+\infty} \frac{k_2k_1}{k_2 - k_1}\frac{J_1(kR)J_1(kr)}{k}\left(\mathrm{e}^{\mathrm{i}k_1 z} - \mathrm{e}^{\mathrm{i}k_2 z}\right)\mathrm{d}k \tag{7.13}$$

and vorticity components

$$\Omega_\alpha = UR\int_0^{\infty} \frac{\mathrm{d}k}{k_2 - k_1}\frac{J_1(kr)J_1(kR)}{k}\left(k_2\mathrm{e}^{\mathrm{i}k_1 z} - k_1\mathrm{e}^{\mathrm{i}k_2 z}\right)\left(k_1k_2 - k^2\right). \tag{7.14}$$

For large distances ($r \gg R$) from the small disk ($R \ll L_\nu, L_\nu = (\nu\Lambda/N)^{1/3}$) in the co-ordinate frame (q, p) connected with the wave cone (axis p is directed normally to the cone) the asymptotic expression for the vertical component of the velocity can be written in canonical form [8]

$$v_z(p,q) = \frac{1-\mathrm{i}}{\sqrt{\pi}}UR^2\sin\theta\sqrt{\frac{\sin\theta}{p\sin\theta + q\cos\theta}}\int_0^{+\infty} k_p^{1/2}\exp\left(\mathrm{i}k_p p - \frac{\nu k_p^3 q}{2N\cos\theta}\right)\mathrm{d}k_p. \tag{7.15}$$

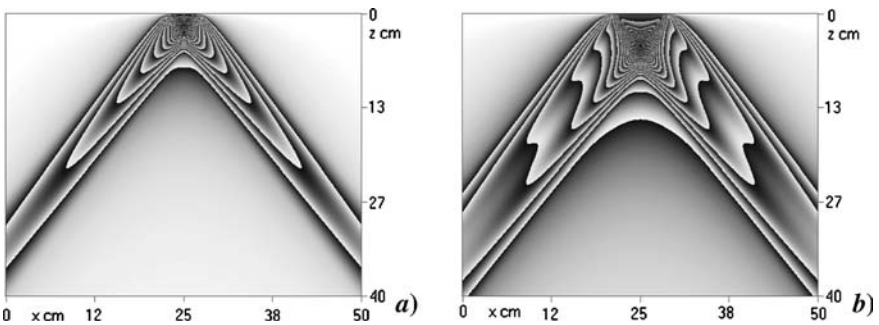

Figure 9. Modal structure in the central plane cross-section of conic 3D periodic waves produced by a vertically oscillating horizontal circular disk of small **a)** – $R = 1.7$ cm, uni-modal; and large **b)** – $R = 4$ cm radius, bi-modal. The field of the vertical velocity component modulus is presented. ($N = 1{\cdot}2\,\mathrm{s}^{-1}$; $\omega = 0{\cdot}998\,\mathrm{s}^{-1}$; $U = 0{\cdot}25$ cm/s, $t = 0$).

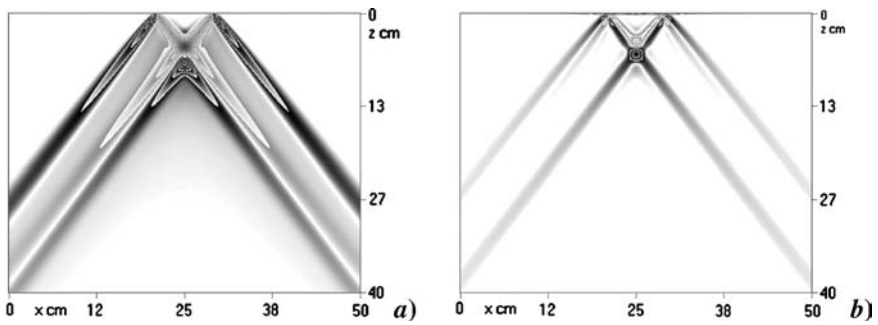

Figure 10. Fine envelopes of a 3D bimodal conic wave-beam produced by a vertically oscillating horizontal circular disk ($N = 1{\cdot}2\,\mathrm{s}^{-1}$; $\omega = 0{\cdot}998\,\mathrm{s}^{-1}$; $U = 0{\cdot}25$ cm/s, $R = 4\,\mathrm{cm} > L_\nu = 1{\cdot}8\,\mathrm{cm}$ $t = 0$) in the fields of derivatives of the radial velocity component: **a)** – first derivative $\partial v_r/\partial z$; **b)** – second derivative $\partial^2 v_r/\partial z^2$.

The wave amplitude decreases inversely proportional to the distance from the source and oscillates across the beam. This expression describes only the regular component of the velocity. For the calculation of singular components the method of boundary functions is used in an ordinary sense.

To illustrate the fine structure of 3D periodic internal waves, the beam integrals (7.6) were calculated numerically on a square mesh with resolution from 0·01 to 0·1 mm. The modal structure of the wave cone is illustrated by Figure 9. A source that is small with respect to the viscous wave-scale L_ν produces a uni-modal symmetric wave-cone; a large generator produces a bi-modal cone that gradually transforms into a uni-modal one with distance.

Asymmetry in the profile of the vertical velocity component reflects the anisotropy of the internal and external edges of the wave cone. The horizontal velocity component is symmetric with respect to the central cone.

Small-scale disturbances on the edges on the beam are clearly visualized by a distribution of first and second derivatives of the radial velocity component. Their thickness is of the order of the magnitude of the thickness of the boundary layer. These elements of the periodic motion are restructured rather fast and during the wave period these disturbances can be distributed across the whole beam or are concentrated in the thin beam envelope. The existence of the fine element of the beam can explain the direct formation of 'trauma stratification' as observed in experiments with crossed periodic internal wave-beams [24, 25] (Figure 10).

Equivalent roots of the same dispersion relation describe all the elements of the family of periodic motions in a continuously stratified fluid. Thus large-scale waves that are regular

elements and small-scale boundary layers that are singular elements are generated and disappear simultaneously. So the time of existence of singular components (boundary layers on rigid surfaces and internal boundary flows on surfaces of discontinuity of the density and its derivatives in the bulk of the fluid) is determined by the time of existence of large-scale waves.

8. Conclusion

This paper describes solutions of fluid-mechanics problems based on an adequate analysis of the governing equations. The analysis is based on calculations of infinitesimal groups, discrete groups and the construction of a complete set of solutions of the linearized problem. If the whole set of regular and supplementing singular components of flow are taken into account, solutions of the initially singularly perturbed problem satisfy all the boundary conditions. Searching for Lie groups was carried out by computer-algebra systems producing well-known calculations that are not easily realized by hand. A new explicit method has been proposed to find discrete symmetry groups for ordinary and partial differential equations and their systems.

Knowledge of the invariants of symmetry groups helps to construct exact solutions of nonlinear differential equations, to find an optimal coordinate frame allowing partial or complete separation of variables, to reduce the number of independent variables or to simplify the governing equations and to calculate regular or asymptotic expansions in a perturbation theory. As to theoretical fluid mechanics, Lie and discrete-group methods help to estimate the degree of mutual reducibility of different models and to find the range of applicability of the governing equations and methods of their solution. Calculations of discrete symmetries allow one to predict and classify possible types of geometric elements of a general flow pattern. Numerous calculations, when applying group-theoretical methods to real fluid-dynamic problems, become feasible due to progress in computer technique and the development of computer-algebraic programs. As an example, the classification of regular cells and rolls produced by Bénard convection in a homogeneous fluid layer has been presented here. Realization of the potentialities of group methods for numerical analysis is a powerful source for further progress in the mathematical description of fluid dynamics with essential reduction of calculation volumes.

The classification of a complete set of 3D periodic motions in fluids presented here generalizes the classical Stokes scheme for waves and accompanying periodic boundary layer. Both internal and acoustic-gravity waves are supplemented by two types of boundary layers on rigid boundaries. The first of these is similar to periodic Stokes flow in a homogeneous fluid, and the second, whose parameters depend both on the buoyancy frequency and the slope of the surface is specific for stratified media. The universal microscale δ_N is the common length scale for both boundary layers.

Inertial acoustic waves in a homogeneous fluid also coexist with two separated boundary layers with distinguished thicknesses. One of these layers is an analogue of the known Ekman layer. An isotropic longitudinal ($\mathbf{v} \| \mathbf{k}$) sound wave in a homogeneous fluid at rest is characterized by the dispersion relation $k^2 = \omega^2 / \left(c^2 - i\omega\left(4\nu/3 + \mu\right)\right)$, which describes waves and a twice degenerated Stokes-type boundary layer of thickness $\delta_\nu = \sqrt{2\nu/\omega}$, where the motion is divergence-free.

Periodic motions in a homogeneous incompressible fluid at rest ($N = g = \Omega = \nabla \cdot \mathbf{v} = 0, c \to \infty$) are characterized by the dispersion relation $\mathbf{k}^2 \left(\omega + \mathrm{i}\nu k^2\right)^2 = 0$, which describes wave-like bi-directional inviscid longitudinal motions ($\mathbf{k}^2 = 0$) with wave-vector components

$\mathbf{v} = -\tilde{P}_0\mathbf{k}/\rho_0$ and a double boundary layer with a thickness $\delta_\nu = \sqrt{2\nu/\omega}$. In the boundary layer transverse, divergence-free isobaric motions are observed ($\mathbf{k}\cdot\mathbf{v} = 0, k_x = (1+\mathrm{i})\sqrt{\omega/2\nu} \quad k_y = k_z = 0$) where $v_x = 0$, and v_y, v_z are independent. Due to the degeneration of 3D boundary layers, the approximation of a homogeneous fluid of constant density (or classical 3D Navier–Stokes equations) is an ill-posed problem.

The inclusion of thermal diffusivity and diffusion in multicomponent media leads to the inclusion of additional equations in the set of governing equations and to an increase in the number of boundary-layer types [16]. A new pair of boundary layers is associated with any additional dissipative parameter. Boundary layers are characterised by completely or partially different scales. Large-scale waves and fine-structure boundary-layer elements are inseparable components of the united system of periodic flows. All elements of this system are generated and disappear simultaneously, regardless of differences in scales. Solutions for stratified rotating media allow a uniform transition to a homogeneous fluid at rest. In this case, two different boundary layers are merged in the unified degenerate layer. The inverse analytic extrapolation of solutions is impossible because of insufficient completeness of the functional space of the original problem.

From an analysis of the exact solution of 3D periodic waves generated by a disk on a solid plane performing small oscillations follows that high-gradient envelopes bound the internal-wave beams in continuously stratified media. The properties of these envelopes and their dynamic impact are needed in further studies.

The sets of governing equations in fluid mechanics form combined systems including nonlinear partial differential equations, a nonlinear algebraic equation of state and boundary conditions on complex solid boundaries mostly having nonlinear shape. The differential equations are characterized by symmetry groups reflecting the basic conservation laws and specific symmetries. Generally, both differential and algebraic parts of the set of governing equations contain small coefficients which can be used for constructing a small expansion parameter and a procedure for simplifying the initially complex and unresolved set, for example introducing the Boussinesq approximation, performing linearization and so on. This operation can essentially change the properties of the studied system. A comparison of the symmetries of the initial and transformed sets of equations helps to estimate the degree of correspondence of these sets.

In the general case, the dynamics of hydrodynamic systems is determined by the nonlinear interaction between all structural flow elements both regular (waves, vortices) and of a singular kind (boundary layers on solid surfaces and internal boundary currents in a fluid interior). In particular, variations in the structure and nonlinear interactions of boundary layers make it possible to generate internal waves, even in the cases where direct excitation is forbidden in a linear theory and by the propagation conditions [3]. Owing to large vorticity, interacting boundary layers are effective generators of vortex motions. Experimental studies of the dynamics of boundary layers and the generation of vortices require substantial improvement of visualization instruments and flow measurement. These instruments must be capable of resolving the fine structure of the smallest flow elements.

Acknowledgements

This work is supported by the Russian Academy of Sciences (Program OE-14 "Dynamic and acoustics of nonhomogeneous fluids, gas–fluid mixtures and suspensions") and by the Russian Foundation for Basic Research (Grants 05-05-64090, 05-01-00154).

References

1. L. D. Landau and E. M. Lifshitz, Course of theoretical physics, In: *Vol. 6: Fluid Mechanics.* Moscow: Nauka (1986) 136 pp; New York: Pergamon (1987).
2. J. Pedlosky, *Geophysical Fluid Dynamics.* 2nd edition. New York: Springer-Verlag (1987) 710 pp.
3. J. Lighthill, *Waves in Fluids*. Cambridge: Cambridge University Press (1978).
4. L. V. Ovsiannikov, *Group Analysis of Differential Equations*. New York: Academic Press (1982).
5. L. V. Ovsiannikov, Programme SUBMODELS. Gas dynamics. *J. Appl. Math. Mech.* 58(4) (1994) 30–55.
6. V. G. Baidulov and Yu. D. Chashechkin, Invariant properties of the equations of motion of stratified fluids. *Dok. Phys.* 47(12) (2002) 888–891. (Translated from *Dokl. Akad. Nauk* 387(6) 760–763.)
7. E. V. Bruyatskii, *Turbulentnye Stratifitsirovannye Struinye Techeniya*. (in Russian, *Turbulent Stratified Jet Flows*). Kiev: Naukova Dumka (1986) 296 pp.
8. W. Rodi, *Turbulence Models and Their Application in Hydraulics – A State of the Art Review*. Karlsruhe: University of Karlsruhe (1980) SBF Report 80/T/125.
9. A. V. Kistovich and Yu. D. Chashechkin, A Regular method of searching for discrete symmetries in models of physical processes. *Dokl. Phys.* 46(10) (2001) 718–721.
10. A. V. Kistovich and Yu. D. Chashechkin, Regular method for searching of differential equations discrete symmetries. *Regular and Chaotic Dynamics* 6(3) (2001) 327–336.
11. A. V. Kistovich and Yu. D. Chashechkin, Types of discrete symmetries of convection in a plane fluid layer. *Dok. Phys.* 47(6) (2002) 458–460. (Translated from *Dokl. Akad. Nauk* 384(5), 630–633.)
12. D. B. White, The planforms and onset of convection with a temperature-dependent viscosity. *J. Fluid Mech.* 191 (1988) 247–286.
13. E. Palm, T. Ellingsen and B. Gjevik, On the occurrence of cellular motion in Benard convection. *J. Fluid Mech.* 30 (1967) 651–661.
14. Yu. D. Chashechkin and A. V. Kistovich, Classification of three-dimensional periodic fluid flows. *Dokl. Phys.* 49(3) (2004) 183–186.
15. Yu. D. Chashechkin and V. V. Mitkin, Experimental study of a fine structure of 2D wakes and mixing past an obstacle in a continuously stratified fluid. *Dyn. Atmosph. Oceans* 34 (2001) 165–187.
16. Yu. D. Chashechkin and A. V. Kistovich, Calculation of the structure of periodic flows in a continuously stratified fluid with allowance for diffusion. *Dokl. Phys.* 48(12) (2003) 710–714.
17. S. A. Gabov and A. G. Sveshnikov, *Zadachi Dinamiki Stratifitsirovannykh Zhidkostei*. (in Russian, *Problems of Stratified Fluids Dynamics*). Moskva: Nauka (1986) 288 pp.
18. Yu. V. Kistovich and Yu. D. Chashechkin, Non-linear generation of periodic internal waves by a boundary-layer flow around a rotating axially symmetric body. *Dokl. Phys.* 44(8) (1999) 573–576.
19. Yu. S. Il'inykh and Yu. D. Chashechkin, Generation of periodic motions by a disk performing torsional oscillations in a viscous continuously stratified fluid. *Fluid Dyn.* 39(1) (2004) 148–161.
20. Yu. V. Kistovich and Yu. D. Chashechkin, A new mechanism of the non-linear generation of internal waves. *Dokl. Phys.* 47(2) (2002) 163–167. (Translated from *Dokl. Akad. Nauk* 382(6) 772–776).
21. Yu. V. Kistovich and Yu. D. Chashechkin, Some exactly solvable problems of the radiation of three-dimensional periodic internal waves. *J. Appl. Mech. Tech. Phys.* 42(2) (2001) 228–236.
22. D. D. Holm and Y. Kimura, Zero-helicity Lagrangian kinematics of three-dimensional advection. *Phys. Fluids* A3 (1991) 1033–1038.
23. A. Yu. Vasiliev and Yu. D. Chashechkin, The generation of beams of three–dimensional periodic internal waves in an exponentially stratified fluid. *J. Appl. Math. Mech.* 67(3) (2003) 397–405.
24. A. D. McEwan and P. A. Plumb, Off-resonant amplification of finite internal wave packets. *Dyn. Atmosph. Oceans* 2 (1977) 83–105.
25. S. G. Teoh, G. N. Ivey and J. Imberger, Laboratory study of the interaction between two internal wave rays. *J. Fluid Mech.* 336 (1997) 91–121.